Geobios 48 (2015) 147–167

Available online at
ScienceDirect
www.sciencedirect.com

Elsevier Masson France
EM|consulte
www.em-consulte.com

Original article

Rhinocerotidae (Mammalia, Perissodactyla) from the chrono-stratigraphically constrained Pleistocene deposits of the urban area of Rome (Central Italy)☆

Luca Pandolfi [a,*], Fabrizio Marra [b]

[a] Università degli Studi Roma Tre, Dipartimento di Scienze, sezione di Geologia, Largo S. L. Murialdo 1, 00146, Roma, Italy
[b] Istituto Nazionale di Geofisica e Vulcanologia, Sezione Roma 1, via di Vigna Murata 605, 00147, Roma, Italy

ARTICLE INFO

Article history:
Received 29 September 2014
Accepted 3 February 2015
Available online 24 February 2015

Keywords:
Stephanorhinus
Coelodonta
Systematics
Chronostratigraphy
Pleistocene
Rome

ABSTRACT

In the present paper we provide a revision of the Pleistocene Rhinocerotidae remains collected so far in the sedimentary deposits of the urban area of Rome. Five Pleistocene species have been identified: *Stephanorhinus etruscus* (Falconer), *Stephanorhinus hundsheimensis* (Toula), *Stephanorhinus hemitoechus* (Falconer), *Stephanorhinus kirchbergensis* (Jäger), and *Coelodonta antiquitatis* (Blumenbach). By establishing correlations of the sedimentary sections hosting the fossil remains with the geochronologically-constrained, astronomically-forced aggradational successions of the Paleo-Tiber River, we frame the fossil remains within a detailed chronostratigraphic scheme with no equivalent in the previous literature. This approach leads to new considerations on the occurrences and paleobiogeography of the recovered species. Based on the studied material, the last occurrence of *S. etruscus* in Italy is here referred to a timespan between 0.86 and 0.82 Ma, thus suggesting a long persistence of this species. Recalibration of the considered deposits enabled us to refer the first evidence of *S. hundsheimensis* in Italy to approximately 0.8 Ma (Ponte Milvio gravels and sands; urban area of Rome). In the Roman area, specimens referred to *S. hundsheimensis* are coeval with relatively smaller and slender remains of an undefined rhinoceros species. *S. hemitoechus* is recorded in fossiliferous deposits earlier than 0.4 Ma and its persistence in the studied area is reported at least until 0.19 Ma. *S. kirchbergensis* occurs for the first time in Italy at ca. 0.56–0.5 Ma (Tor di Quinto deposit; urban area of Rome) and persists in the considered area until 0.37–0.29 Ma. *C. antiquitatis* is here reported for the first time within the Roman area, so adding a new record of this species in Italy. Unfortunately, the exact locality in which the specimens were collected is unknown, preventing from precise chronostratigraphic assessment.

1. Introduction

The knowledge of the chronology of different faunal assemblages, as well as those of different taxa, is significant for the paleobiogeography, paleoecology, and evolutionary history understanding of any fossil species. Nevertheless, terrestrial fossil remains are usually collected in continental deposits in which chronostratigraphic constraints are lacking or uncertain. When available, several methodologies (e.g., pollen analysis, magnetochronology, biochronology, geochemical analysis) are therefore used to obtain an absolute or relative chronology of the different findings (Ravazzi et al., 2005; Muttoni et al., 2009; Palombo et al., 2010; Petronio et al., 2011; Pandolfi et al., 2013a). In the present study, we apply a method of correlation of the sedimentary successions with the astronomically-forced, glacial sea-level oscillations (Marra et al., 2008), which has revealed particularly useful for biostratigraphic studies in the coastal area of Rome (Marra et al., 2014a), to perform a revision of the Pleistocene rhinoceros collected in the urban area of Rome (Fig. 1). By reviewing the taxonomy of the considered remains and by correlating the fossiliferous deposits in which they were collected with the Marine Isotopic Stages (MIS), we assess their age and discuss the consequent paleobiological implications of this newly established chronology.

2. Stratigraphic framework of the investigated area

The Roman area is among the most important sedimentary basins in Europe based on its richness in fossil mammal remains

☆ Corresponding editor: Pierre-Olivier Antoine.

* Corresponding author.
E-mail address: luca.pandolfi@uniroma3.it (L. Pandolfi).

http://dx.doi.org/10.1016/j.geobios.2015.02.003
0016-6995/

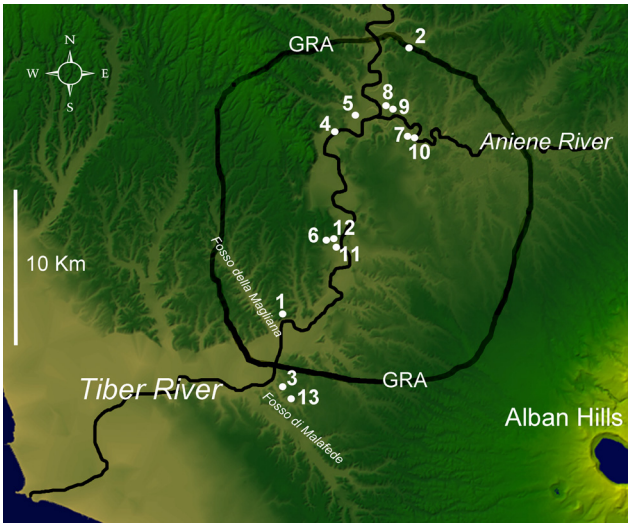

Fig. 1. Location of the fossiliferous localities within the urban area of Rome mentioned in the text. **1**: Monte delle Piche; **2**: Cava Redicicoli; **3**: Vitinia; **4**: Ponte Molle; **5**: Tor di Quinto; **6**: Monte Verde; **7**: Sedia del Diavolo; **8**: Monte Sacro; **9**: Prati Fiscali; **10**: Batteria Nomentana; **11**: Vigna San Carlo; **12**: Vigne Torte; **13**: Fosso di Malafede.

(Ambrosetti, 1967; Petronio and Sardella, 1999; Palombo, 2004; Milli and Palombo, 2005; Kotsakis and Barisone, 2008; Petronio et al., 2011; Marra et al., 2014a), and due to a number of stratigraphic studies (Marra and Rosa, 1995 and references therein) performed since the end of the 19th century. This area hosted the delta of the Paleo-Tiber River since the Middle Pleistocene through the Present; its evolution is the result of complex geological processes, which included tectonics, volcanism and glacio-eustatic fluctuations (Karner et al., 2001a). The continental to coastal sedimentary successions of the Paleo-Tiber River were deposited since 800 ka in response to sea-level rise during the Pleistocene glacial terminations, as demonstrated by a series of recent studies, which using the $^{40}Ar/^{39}Ar$ ages of tephra intercalated within the sedimentary deposits provided geochronologic constraints linking these aggradational successions to the different MIS (Karner and Renne, 1998; Karner and Marra, 1998; Marra et al., 1998; Florindo et al., 2007; Marra and Florindo, 2014). The aggradational successions in the area of Rome are therefore a discontinuous stratigraphic record, constituted by a succession of ten major aggradational units deposited during MIS 22-21 through MIS 2-1, plus several minor successions corresponding to more pronounced sub-stages, representing the physical remnant of as many glacio-eustatic sea-level cycles in this timespan. These aggradational successions fill the fluvial valleys and the coastal plain incisions that were excavated during the periods of sea-level lowstand, and interfinger with the pyroclastic products of the Colli Albani and Monti Sabatini Volcanic Districts, whose paroxismal activity spanned 600–250 ka (Marra et al., 2009, 2014b). It is noteworthy that the majority of the Middle Pleistocene fossil vertebrates assemblages of Italy have been sampled in the Roman area in these alluvial deposits of the Paleo-Tiber River and its tributaries (Fig. 1; Caloi et al., 1998; Di Stefano et al., 1998; Milli et al., 2004; Petronio et al., 2011), exposed by continuous tectonic uplift affecting this area (Karner et al., 2001a). A large number of vertebrate fossil remains were collected from the deposits cropping out in the area of Rome due to the intense urbanisation and quarry activities (e.g., Meli, 1896; Ponzi, 1878; Portis, 1896). These remains are mainly stored at the Museo di Paleontologia, Sapienza, University of Rome and were already mentioned in several contributions (e.g., Caloi et al., 1998; Di Stefano et al., 1998; Palombo et al., 2002; Kotsakis and Barisone, 2008; Pandolfi, 2011a, 2013). However, most of them lack of precise stratigraphic constraints since their finding is referred to a locality and, not always, is associated to a generic sedimentary level (gravel, sand, clay, etc.), preventing their direct correlation with a chronostratigraphic unit. In order to provide such correlation, in the present work we apply the method of correlation with the geochronologically-constrained aggradational units of the Paleo-Tiber described in Marra et al. (2014a). Based on this approach, any fossil that can be referred to an identified geochronologically-constrained sedimentary unit can be assigned a discrete age, corresponding to that of the associated MIS (Fig. 2). Identification of the glacio-eustatically forced sedimentary units can be achieved by:

- literature data, whenever the outcrop corresponds to published type-sections;
- the stratigraphic context, whenever the stratigraphic position of the outcrop with respect to other dated sections is determinable;
- recognition of pyroclastic deposits of known age within the outcrop.

3. Material and methods

The revised Quaternary time scale (Gibbard et al., 2010) is used for chronological references in this text. Therefore, the Pliocene spans approximately between 5.4 Ma and 2.6 Ma. The age of the sedimentary deposits hosting the fossil remains was established based on correlation with the geochronologically-constrained aggradational successions of the Paleo-Tiber, as summarized in Fig. 2 and Table 1. The time of deposition was therefore referred to an interval corresponding with a portion of the Oxygen Isotopes curve, indicated by the correspondent MIS(s) or, when available, by the $^{40}Ar/^{39}Ar$ age of tephra layers intercalated in the sedimentary deposit. All the radioisotopic ages in this paper were calculated according to the age of 28.201 Ma for the Fish Canyon Tuff sanidine standard (Kuiper et al., 2008).

The fossil specimens from the urban area of Rome are housed at Museo di Paleontologia, Sapienza, University of Rome (MPUR) and Museo di Geologia "Giovanni Capellini", Bologna (MGGC); they were mainly collected during the end of the 19th century and the beginning of the 20th century (Table 1). The specimens were morphologically compared with several Pliocene and Pleistocene remains referred to *Coelodonta antiquitatis* (Blumenbach, 1799), "*Dihoplus*" *megarhinus* (De Christol, 1834), *Stephanorhinus kirchbergensis* (Jäger, 1839), *S. hemitoechus* (Falconer, 1859), *S. etruscus* (Falconer, 1868), *S. hundsheimensis* (Toula, 1902), and *S. jeanvireti* (Guérin, 1972). These specimens were collected from a number of European localities and are currently housed in several European institutions. The morphometric methodology follows that introduced by Guérin (1980) and Fortelius et al. (1993); the anatomical descriptions and the dental terminology follow those of Guérin (1980) and Antoine (2002).

Institutional Abbreviations: **BSPG**, Bayerische Staatssammlung für Paläontologie und Geologie, Munich, Germany; **HNHM**, Hungarian Natural History Museum, Budapest, Hungary; **IGF**, Museo di Storia Naturale, sezione di Geologia e Paleontologia, Florence, Italy; **IQW**, Institute für Quartärpaläontologie, Weimar, Germany; **MFGI**, Geological and Geophysical Institute of Hungary, Budapest, Hungary; **MfN**, Museum für Naturkunde, Berlin, Germany; **MGGC**, Museo di Geologia Giovanni Capellini, Bologna, Italy; **MGPP**, Museo di Geologia e Paleontologia, Padua, Italy;

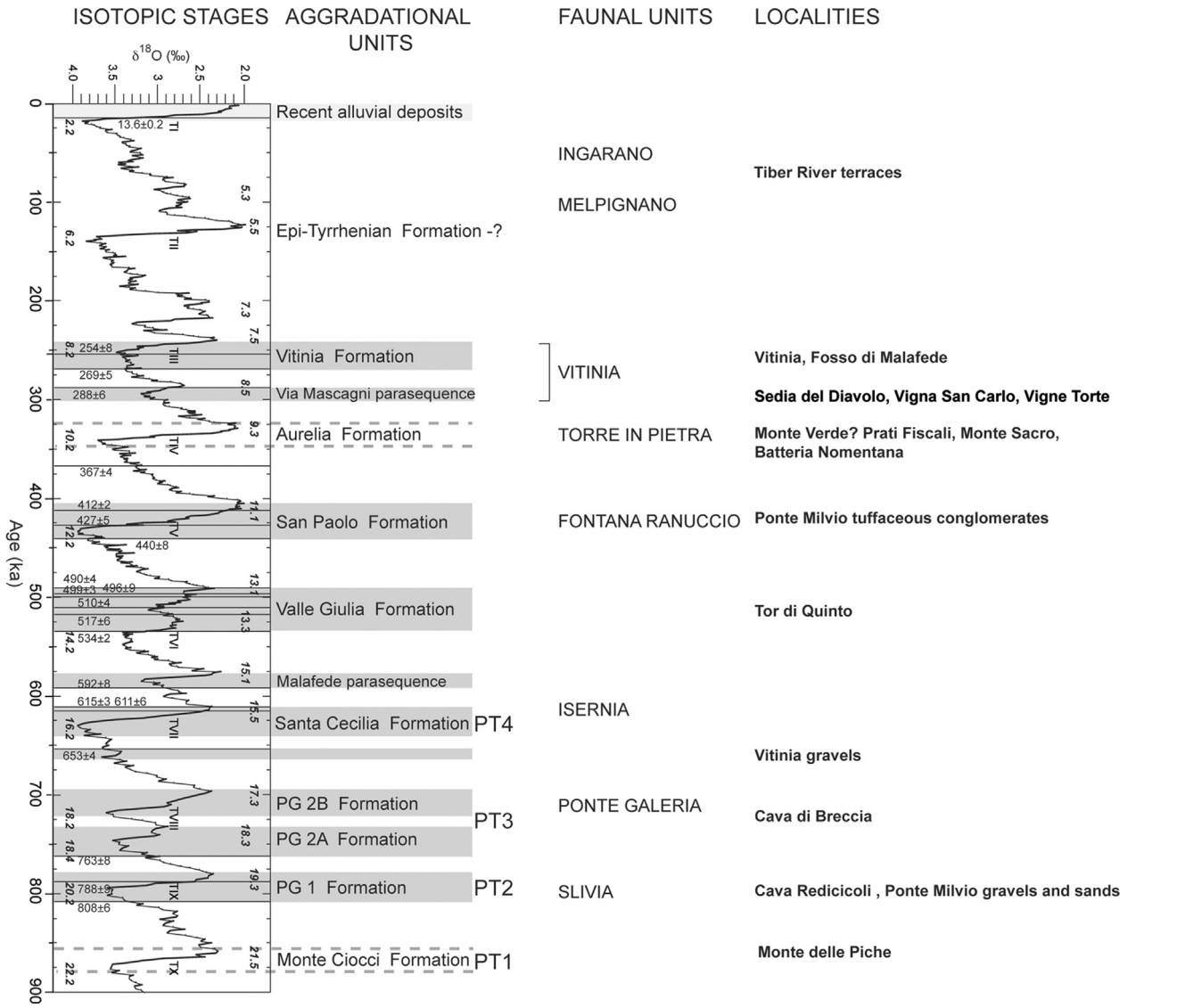

Fig. 2. Attribution to the geochronologically-constrained aggradational units of the Paleo-Tiber River (see Marra et al., 2014a and references therein) of the sedimentary deposits cropping out at the localities where the fossil remains revised in this work occur, providing their correlation with the $\delta^{18}O$ isotopic record timescale (Lisiecki and Raymo, 2005). Horizontal lines are the age constraints derived by the $^{40}Ar/^{39}Ar$ dating of the volcanic deposits intercalated within the aggradational units of the Paleo-Tiber River (Karner and Renne, 1998; Karner et al., 2001b; Florindo et al., 2007; Marra et al., 2014a). Each shaded box individuates a period of sea-level rise that accounts for the deposition of the sedimentary successions in the coastal area of Rome. Periods of sea-level rise for which radiometric age constraints to the sedimentary succession are not available are bounded with dashed lines.

MNCN, Museo Nacional de Ciencias Naturales, Madrid, Spain; **MNHM**, Naturhistorisches Museum, Mainz, Germany; **MNHN**, Muséum National d'Histoire Naturelle, Paris, France; **MNPELP**, Museo Nazionale Preistorico Etnografico Luigi Pigorini, Rome, Italy; **MPAVC**, Paleontological and Archaeological Museum "Virginio Caccia", San Colombano al Lambro, Milan; **MPLBP**, Museo di Paleontologia "L. Boldrini", Pietrafitta, Perugia, Italy; **MPM**, Museo Paleontologico di Maglie, Lecce, Italy; **MPP**, Museo di Paleontologia, Università di Parma, Parma, Italy; **MPUR**, Museo di Paleontologia, Sapienza, University of Rome, Rome, Italy; **MSNAF**, Museo di Storia Naturale, Accademia dei Fisiocritici, Siena, Italy; **MSNF**, Museo di Storia Naturale, sezione di Zoologia, Florence, Italy; **MSTB**, Museo di Scienze della Terra, University of Bari, Bari, Italy; **NHML**, Natural History Museum, London, England; **NHMW**, Naturhistorisches Museum, Wien, Austria; **NMB**, Naturhistorisches Museum, Basel, Switzerland; **SMNK**, Staatliches Museum für Naturkunde, Karlsruhe, Germany; **SMNS**, Staatliches Museum für Naturkunde, Stuttgart, Germany.

4. Results

4.1. Description and comparison of Rhinocerotidae remains from the urban area of Rome

4.1.1. Monte delle Piche

Three mandibles (MPUR 1515; MPUR 1516; MPUR 138) have been collected from the marine deposits of Monte delle Piche (Ponzi, 1858; Pandolfi et al., 2013b, 2015). The rhino mandible MPUR 138 was discussed by Portis (1899), who refers it to *Dicerorhinus schleiermacheri* (Kaup, 1832), and by Guérin (1980), who considers it as *Chilotherium* Ringström, 1924. However, according to Pandolfi et al. (2013b), the morphology of the mandible MPUR 138 is close to that of *Acerorhinus* Kretzoi, 1942 (the symphysis is robust and narrow and begins curving upwards below p2, there is no indication of any alveolus for i1, the alveoli of the i2 are very close to each other and the right tusk curves strongly upwards, the horizontal ramus of the mandible is deep and displays an uniform height), and the

Table 1
Taxonomy, locality and age of the specimens collected from the urban area of Rome and included in this work.

Locality	Lithofacies	Age (in Ma) or MIS	Taxon	Specimen
Monte delle Piche	Marine deposits	0.86–0.82	*Stephanorhinus* sp.	MPUR 1515
Monte delle Piche	Marine deposits	0.86–0.82	*Stephanorhinus etruscus*	MPUR 1516
Monte delle Piche	Marine deposits	0.86–0.82	*Acerorhinus* sp. (reworked element)	MPUR 138
Cava Redicicoli	Fluvial gravels	0.81–0.79	*Stephanorhinus* sp.	MPUR 1956R45
Cava Redicicoli	Fluvial gravels	0.81–0.79	*Stephanorhinus hundsheimensis*	MPUR 1956R2, MPUR 1956
Ponte Molle	Gravel and sands	0.81–0.79	*Stephanorhinus hundsheimensis*	MPUR 1420-97, MPUR 1454-117, MPUR 1454-118, MPUR 1412-8
Ponte Molle	Gravel and sands	0.81–0.79	*Stephanorhinus* aff. *hundsheimensis*	MPUR 1523-2
Vitinia	Gravel and sands	0.65–0.62	*Stephanorhinus* aff. *hundsheimensis*	MPUR 9/3 ex 2768
Tor di Quinto		0.56–0.50	*Stephanorhinus* sp.	MPUR 1447-123, MPUR 1455-87, MPUR 1455-86
Tor di Quinto		0.56–0.5	*Stephanorhinus kirchbergensis*	MPUR 1458-54, MPUR 1425-99
Tor di Quinto		0.56–0.5	*Stephanorhinus* sp.	MPUR 1424-44
Tor di Quinto		0.56–0.5	*Stephanorhinus* sp.	MPUR 1457-108
Tor di Quinto		0.56–0.5	Rhinocerotidae	MPUR 1425-98
Ponte Molle	Tufaceous conglomerates	0.46–0.43	*Stephanorhinus* cf. *hemitoechus*	MPUR 1439-134, MPUR 1448-51
Ponte Molle	Tufaceous conglomerates	0.46–0.43	*Stephanorhinus kirchbergensis*	MPUR 1417-115, MPUR 1456-126, MPUR 1415-63
Monte Verde		0.37–0.33	*Stephanorhinus* sp.	MPUR 1422-61
Sedia del Diavolo	Clay level	0.37–0.29	*Stephanorhinus* sp.	MPUR?
Sedia del Diavolo	Upper gravels	0.37–0.29	*Stephanorhinus* sp.	MPUR?
Sedia del Diavolo	Upper gravels	0.37–0.29	*Stephanorhinus hemitoechus*	MPUR?
Monte Sacro	Tufaceous conglomerates	0.37–0.29	*Stephanorhinus hemitoechus*	MPUR 1497, MPUR 1497a, MPUR 1426-106, MPUR 1510
Monte Sacro	Tufaceous conglomerates	0.37–0.29	*Stephanorhinus* sp.	MPUR 1427-31, MPUR 1428-24, MPUR 1478-91
Prati Fiscali		0.37–0.29	*Stephanorhinus* sp.	MPUR 1476-105, MPUR 1471
Batteria Nomentana	Levels covering the "Tufo Litoide Lionato"	0.37–0.29	*Stephanorhinus* sp.	MPUR 1477-68
Vigna San Carlo		0.37–0.29	*Stephanorhinus hemitoechus*	MPUR 1514-148
Vigna San Carlo		0.37–0.29	*Stephanorhinus* sp.	MPUR 1501-28
Vigne Torte	Gravels underlie tufs	0.37–0.29	*Stephanorhinus hemitoechus*	MPUR 1489-111
Vigne Torte	Gravels underlie tufs	0.37–0.29	*Stephanorhinus* sp.	MPUR 1470-76, MPUR 1474-48
Vigne Torte	Gravels underlie tufs	0.37–0.29	Rhinocerotini indet.	MPUR 1469-93
Vitinia	Upper levels	0.25–0.19	*Stephanorhinus hemitoechus*	MPUR V2766
Fosso di Malafede		0.25–0.19	*Stephanorhinus hemitoechus*	MPUR V2832
Rome, Tiber river terraces		MIS 4–3?	*Coelodonta antiquitatis*	MGGC33, MGGC nn
Rome, urban area, undefined locality		–	*Stephanorhinus kirchbergensis*	MPUR 1498 in pars
Rome, urban area, undefined locality		–	*Stephanorhinus kirchbergensis*	MPUR 1499 in pars
Rome, urban area, undefined locality		–	*Stephanorhinus kirchbergensis*	MPUR 1518, MPUR 1519

specimen is a reworked Miocene element in Pleistocene deposits (Pandolfi et al., 2013b, 2015).

The specimen MPUR 1515 consists only of a partial horizontal ramus with dp3, dp4 and m1; it is covered by a thick and hard crust of sediment (Pandolfi et al., 2015). The lingual valleys of the teeth have a V-shaped morphology, labial cingula are absent, dp4 and m1 display a relatively marked and deep vestibular grooves. These features are recognised in dp4 and m1 of *S. etruscus* from Pirro Nord (MPUR) and Barberino di Mugello (MGGC), as well as in the specimens of *S. etruscus* reported by Lacombat (2006). In dp3 from Monte delle Piche, the vestibular groove is open and shallow as in dp3 of *S. etruscus* from Castel San Pietro (MPUR). The specimen MPUR 1515 differs from *S. hundsheimensis* from Mosbach (MfN) in which the vestibular wall of the trigonid in dp3 is slightly concave and dp4 has an U-shaped posterior lingual valley and a deep vestibular groove. Two dp4 of *S. hundsheimensis* from Contrada Monticelli (MSTB) display a more obtuse and shallow vestibular groove as well as in the specimens of *S. hundsheimensis* reported by Lacombat (2006). In "*Dihoplus*" *megarhinus* (NMB), dp3 has a relatively more marked and deep vestibular groove than in the Monte delle Piche specimen, dp3 and dp4 display distal and mesial cingula. Unfortunately, the deciduous teeth of *S. jeanvireti* do not show distinctive morphological and morphometric features (Guérin, 1972, 1980) and an exhaustive comparison is prevented. The specimen MPUR 1515 is therefore referred as *Stephanorhinus* sp (Pandolfi et al., 2015).

The almost complete mandible MPUR 1516 displays a regularly convex ventral border of the horizontal ramus; labial cingula are absent, and the lingual valleys have a V-shaped morphology in all the teeth (Pandolfi et al., 2015). The mandible MPUR 1516 differs from those of "*D.*" *megarhinus* from Montpellier (NMB) in which the lower border of the mandible below the molar portion is linear and an inflexion point is present at the level of m1. Furthermore, the lingual valleys in "*D.*" *megarhinus* have usually a U-shaped morphology (Guérin, 1980). In *S. jeanvireti* (MGC, IGF, NMB), the lower border of the mandible appears less convex than in the specimen from Monte delle Piche; moreover, weak vestibular cingula can be recognised on the teeth of *S. jeanvireti* (Pandolfi et al., 2015). The mandible MPUR 1516 differs from those of *S. hundsheimensis* (MPI, MSTB, MPP, NHMW), which display a more slender mandible with a straight ventral border. In *S. etruscus* from Upper Valdarno and Olivola (IGF, NMB), mesial cingula occur in m2 and m3, while vestibular cingula are generally absent or are represented by a more or less marked extension of the mesial cingulum. In *S. etruscus* from Upper Valdarno (IGF, NMB), the lower border of the mandible is regularly convex, as well as in the specimen from Monte delle Piche (Pandolfi et al., 2015). Consequently, the specimen MPUR 1516 is ascribed to *S. etruscus*.

4.1.2. Cava Redicicoli

Three specimens are housed at MPUR: one fragmentary skull (1956 sn), one isolated M1 (1956 R2), and one fragmentary mandible (1956 R45) (Tables 2–5). These remains were ascribed to *Dicerorhinus* sp. by Caloi et al. (1979) (*Rhinoceros* sp. in Blanc, 1955) and were later reported as *S. hundsheimensis* (Caloi and Palombo, 1988; Di Stefano et al., 1998; Milli and Palombo, 2005; Pandolfi and Petronio, 2011).

Table 2
Morphometric comparisons between the skulls collected within the urban area of Rome and *S. etruscus*, *S. hundsheimensis*, *S. hemitoechus*, *S. kirchbergensis* and *C. antiquitatis*.

Skull	Specimen	TDf	TDOC	HOC-F	TDM	TDpc	TDc
Cava Redicicoli	MPUR 1956	ca. 45	137	150	215.3	67	–
Tiber Terrace	MGGC nn	66.42	204.68	164.53	225.15	68.87	162.6
Fosso di Malafede	MPUR v2832	52	134	–	270	125	133
S. etruscus	min–max	40–57.5	101–174	117–153	158–228	34–60.5	79–126
S. hundsheimensis	min–max	49.5–63	132–175	139–191.5	132–175	35–88	107–145
S. hemitoechus	min–max	37–61.5	101–160	141–186	220–288	18–70	107–138
S. kirchbergensis	min–max	49–61.5	131–167	155–178	252–275	57–62	125–149
C. antiquitatis	min–max	43–76	150–275.5	141.5–208	245–313	53–163.5	111–144.5

Data from Guérin, 1980.
All dimensions are in mm. TDf: transverse diameter of the foramen magnum; TDOC: transverse diameter of the occipital crest; HOC-F: height of the occipital face, from the dorsal border of the foramen magnum to the dorsal border of the occipital crest; TDM: transverse diameter at the level of the mastoid apophyses; TDpc: minimal distance between the frontal-parietal crests; TDc: transverse diameter of the postorbital constriction.

Table 3
Morphometric comparisons between the mandibles collected within the urban area of Rome and *S. etruscus*, *S. hundsheimensis*, *S. hemitoechus*, *S. kirchbergensis* and *C. antiquitatis*.

Mandible	Specimen	HC-VB	HS	DAPAR	Lm3/G	Hm1/m2	Hm2/m3	Hm3
Cava Redicicoli	MPUR 1956 R45	–	–	–	–	83	78	–
Vigna San Carlo	MPUR 1514-148	240	207	142	175	92	92	84
S. etruscus	min–max	182–243	–	115–152	–	64–91	70–96.5	79–105
S. hundsheimensis	min–max	230–292	–	128–169	–	78–105	78–104	79–108
S. hemitoechus	min–max	232–272	–	133–164	–	70–110	75–115	79–124
S. kirchbergensis	min–max	235–300	–	158–193	–	90–117	93–125	100–125
C. antiquitatis	min–max	200–334	–	127–202	–	74–124	79–126	83–122

Data from Guérin, 1980.
All dimensions are in mm. HC-VB: height of the vertical ramus (articular condyle-ventral border of the mandible); HS: height of the sigmoid incisure; DAPAR: antero-posterior diameter of the vertical ramus at the level of the toothrow; Lm3/G: length from the distal border of m3 to the posterior border of the vertical ramus; Hm1/m2: height of the horizontal ramus at the level of m1/m2; Hm2/m3: height of the horizontal ramus at the level of m2/m3; Hm3: height of the horizontal ramus at the level of m3.

Table 4
Measurements (in mm) of the upper teeth collected within the urban area of Rome.

Locality	Specimen	Tooth	LL	BL	MW	DW
Cava Redicicoli	MPUR 1956R2	M1	40.2	48	57	50
Ponte Molle	MPUR 1420-97	P4	34.75	39.85	51.75	49.2
Ponte Molle	MPUR 1454-117	M3	52	65	58	–
Ponte Molle	MPUR 1454-118	M3	51	–	57	–
Ponte Molle	MPUR 1439-134	P3	ca. 28	ca. 28	ca. 41	ca. 42
Ponte Molle	MPUR 1417-115	M2	–	62	76	–
Tor di Quinto	MPUR 1447-123	P4	ca. 34	–	–	45
Tor di Quinto	MPUR1457-108	P3	24	28.5	39	37
Tor di Quinto	MPUR 1425-98	DP3?	30	33	46	40
Tor di Quinto	MPUR 1425-99	DP3	32	40	48	44
Monte Sacro	MPUR 1497	P2	18	30	31	34
Monte Sacro	MPUR 1498	P3	29	34.5	42	44
Monte Sacro	MPUR 1499	P4	35	39.5	52	51
Monte Sacro	MPUR 1500	M1	ca. 41	ca. 52	62	ca. 54
Monte Sacro	MPUR 1501	M2	ca. 44	56	ca. 48	62
Monte Sacro	MPUR 1502	M3	ca. 52	70	–	–
Monte Sacro	MPUR 1497a	P2	19	30	30	34
Monte Sacro	MPUR 1497a	P3	ca. 30	ca. 35	43	46
Monte Sacro	MPUR 1497a	P4	ca. 35	41	53	52
Monte Sacro	MPUR 1497a	M1	ca. 43	–	–	–
Monte Sacro	MPUR 1497a	M2	–	55	–	–
Monte Sacro	MPUR 1428-24	M3	ca. 50	–	ca. 57	63
Monte Sacro	MPUR 1427-31	M3	52	–	55.2	64
Monte Sacro	MPUR 1426-106	M2	42.5	62.5	62	46
Monte Sacro	MPUR 1478-91	M3	47	–	54	57.2

LL: lingual length; BL: buccal length; MW: mesial width; DW: distal width.

The fragmentary skull (1956 sn) displays, in lateral view, a straight occipital face; in the same view, the occipital crest does not extend much posteriorly. The dorsal profile of the skull is slightly concave and the Zeuner's angle n is approximately of 170°. The external auditory pseudomeatus is ventrally closed. In dorsal view, the frontal-parietal crests are marked and distant, and the posterior border of the occipital crest has a shallow concavity in the middle. In occipital view, the occipital face is bell-shaped, and the dorsal border of the occipital crest is convex. In basioccipital view, the foramen nervi hypoglossi is shifted antero-externally and a sagittal crest is present on the basilar process. *Stephanorhinus etruscus* (IGF, NMB) differs from the considered specimen in having, in occipital view, a rectangular shape of the occipital face and a straight dorsal border of the occipital crest. In *S. kirchbergensis* (MNHN, NMB, SMNK, SMNS), the occipital crest extends less posteriorly than the occipital condyles, the dorsal profile of the skull is more concave, the occipital face is subtrapezoidal, and the occipital crest is straight in occipital view. The skulls of *S. hemitoechus* (NHML, NMB, IGF, MPUR, MPP, MPAVC) are generally larger than that from Cava Redicicoli, and are

Table 5
Measurements (in mm) of the lower teeth collected within the urban area of Rome.

Locality	Specimen	Tooth	LL	BL	MW	DW	Lmax	Wmax
Cava Redicicoli	MPUR 1956 R45	m1	–	38.5	–	–	–	–
Cava Redicicoli	MPUR 1956 R45	m2	41	42.5	24	27	–	–
Ponte Molle	MPUR 1412-8	m1	46.13	45.05	25.85	27.65	–	–
Ponte Molle	MPUR 1448-51	dp4	36.9	37.5	19.45	21.73	–	–
Ponte Molle	MPUR 1415-63	m3	50	45	26	33	–	–
Tor di Quinto	MPUR 1424-44	dp3	37	40	19	22	–	–
Tor di Quinto	MPUR 1458-54	p2	24	26	–	19	–	–
Tor di Quinto	MPUR 1455-87	p3	–	33	20	–	–	–
Tor di Quinto	MPUR 1455-86	p4	44	44	21	23	–	–
Vigna San Carlo	MPUR 1501-28	dp1	–	–	–	–	(19)	(15)
Vigna San Carlo	MPUR 1501-28	dp2	–	–	–	–	(31)	(20)
Vigna San Carlo	MPUR 1501-28	dp3	–	–	–	–	(42)	(27)
Vigna San Carlo	MPUR 1501-28	dp4	–	–	–	–	(43)	(30)
Vigna San Carlo	MPUR 1514-148	m1	40.5	40	26	28.5	–	–
Vigna San Carlo	MPUR 1514-148	m2	ca. 45	50	ca. 31	ca. 28	–	–
Vigna San Carlo	MPUR 1514-148	m3	49	45	28	27	–	–
Batteria Nomentana	MPUR 1477-68	m3	51	49.5	28	27	–	–
Monte Verde	MPUR 1422-61	m1	39	38	25	30	–	–
Monte Verde	MPUR 1422-61	m2	44	40	25	29.5	–	–

LL: lingual length; BL: buccal length; MW: mesial width; DW: distal width; Lmax: maximal length; Wmax: maximal width.

characterised by a well-developed occipital crest, which extends more posteriorly than the occipital condyles. Moreover, in *S. hemitoechus*, the occipital crest is usually straight in dorsal view with a bulge in the middle and has a straight dorsal profile in occipital view. The overall morphology of the fragmentary skull from Cava Redicicoli resembles that of *S. hundsheimensis* from Hundsheim (NHMW), which is characterised, in occipital view, by a convex dorsal profile of the occipital crest, a bell-shaped occipital face, a shallow concavity in the middle of the occipital crest in dorsal view, and a slightly concave dorsal profile of the skull.

M1 (1956 R2) is relatively worn, the ectoloph profile has a slightly marked paracone fold, the crochet is single, the mesial cingulum is present, and the lingual cingulum is absent. On the whole, the specimen morphologically resembles the M1s of *S. hundsheimensis* from Hundsheim (NHMW 1909.11.598 and 2013/0282/0001). *S. kirchbergensis* differs from the tooth of Cava Redicicoli in having shallow folds and styli on the ectoloph and lingual cusps bulbously inflated (MPUR, NHML, MfN). In *S. hemitoechus* (IGF, MNCN, MPUR, NHML, NMB), the paracone fold is usually more marked than in the studied specimen and the crista is usually present also in an advanced stage of tooth-wear. In addition, the crown is relatively higher in *S. hemitoechus* than in the considered specimen.

The fragmentary mandible (1956 R45) displays only a part of the horizontal ramus with m1 and m2. The portion of the horizontal ramus is relatively low. The molars are much worn and m1 is damaged. The lingual cingulum occurs below the lingual valleys on m2 and the difference in height between the bottoms of the valleys is small in this tooth. The morphological characters of the specimen are not sufficient for a safe specific attribution.

4.1.3. Vitinia, gravels and sands

The third metacarpal (MPUR 9/3 ex 2768: Fig. 3(A, B)) collected at Vitinia was ascribed to *S.* cf. *hemitoechus* by Caloi et al. (1981). In anterior view, the proximal-lateral tuberosity is prominent and the proximal border of the proximal articular surface is concave (Fig. 3(B)). The angle between the lateral border of the diaphysis and the lateral border of the proximal tuberosity is very obtuse. In proximal view, the articular surface for the magnum is sub-trapezoidal, with a straight medial border and a slightly straight anterior border (Fig. 3(A)). This surface is separated from a smaller surface for the uncinate by a strong saliency. In lateral view, the anterior-proximal and the posterior articular surfaces are separated by a bland groove. The anterior-proximal surface is small, subelliptical, and proximally joined with that for the uncinate. The posterior articular surface is large and subtriangular in shape.

On the third metacarpal of *S. etruscus* from Upper Valdarno (IGF) and Senèze (NMB), the posterior articular surface on the proximal epiphysis is subelliptical and it is separated from the anterior one by a marked groove. In addition, the posterior-lateral surface is flat on the studied specimens of *S. etruscus* whereas it is proximal-distally concave on the specimen from Vitinia. The latter can be distinguished from *S. kirchbergensis* from Taubach (NMB), Hornerberg (NMB) and Grays (NHML), which displays a little developed anterior-lateral tuberosity on the proximal epiphysis and a more obtuse angle between the lateral border of the diaphysis and that of the tuberosity. Moreover, in lateral view, the anterior-proximal articular surface is large and separated from the posterior one by a marked groove. The proximal epiphysis of the specimen from Vitinia is smaller than *S. hemitoechus* (MNPELP, MNCN, NHML, MPUR). The latter species displays a more rounded posterior-lateral articular surface in the proximal epiphysis and a marked groove between the two articular surfaces for the fourth metacarpal. Moreover, the anterior-lateral surface is placed higher on the proximal epiphysis in *S. hemitoechus*. Compared with *S. hundsheimensis* from Hundsheim (NHMW), the specimen from Vitinia is slender, the anterior-lateral tuberosity on the proximal epiphysis is less massive, and the proximal articular surface is less transversally wide. The dimensions of the specimen from Vitinia fall into the ranges of *S. etruscus* and *S. hundsheimensis* given by Guérin (1980) and partially in those of *S. hemitoechus* (Table 6). In particular, the length, the proximal transverse diameter, and the transverse and antero-posterior diameters of the diaphysis are close to the minimal values of both *S. etruscus* and *S. hundsheimensis* (Table 6). Accordingly, the specimen is provisionally referred to *Stephanorhinus* aff. *hundsheimensis* because it slightly resembles *S. hundsheimensis* in morphology rather than *S. etruscus*.

4.1.4. Ponte Molle (= Ponte Milvio), gravels and sands levels

Several rhinoceros remains have been collected from the gravels and sands of Ponte Molle (Di Stefano et al., 1998; Pandolfi, 2013; Tables 4 and 5). The specimens have been recently described by Pandolfi (2013), who referred them to *S. hundsheimensis* and *S.* aff. *hundsheimensis*.

Fig. 3. *Stephanorhinus* aff. *hundsheimensis* from the urban area of Rome. **A, B**. Third metacarpal (MPUR 9/3 ex 2768) from Vitinia gravels and sands, in proximal (A) and anterior (B) views. **C, D**. Proximal half of femur (MPUR 1523-2) from Ponte Molle gravels and sands, in proximal (C) and anterior (D) views. Scale bars: 5 cm.

The P4 (MPUR 1420-97) displays a double crochet and mesial and lingual cingula; the ectoloph profile has a slight salient paracone fold (Pandolfi, 2013). These morphological characters are evident in *S. hundsheimensis* from Hundsheim (NHMW) and other localities. In *S. hemitoechus* the paracone fold is marked, the metacone fold is evident (and the profile of the ectoloph is wavy), the lingual cingulum is less developed. P4s of *S. kirchbergensis* from Grays and Taubach have a subtrapezoidal shape and display a less developed and oblique lingual cingulum.

On two M3 (MPUR 1454-117 and MPUR 1454-118) crista and antecrochet are absent and the mediofossette is open. The mesial cingulum is present in both teeth and a vertical style is observed on the median valley of MPUR 1454-117 (Pandolfi, 2013). The ectoloph profile is slightly convex and the paracone fold is slightly marked on MPUR 1454-118. M3s of *S. hemitoechus* and *S. kirchbergensis* usually display a closed mediofossette; the paracone fold is marked on M3s of *S. hemitoechus*.

On m1 (MPUR 1412-8) the anterior and posterior valleys have a V-shaped morphology; the difference in height between the bottom of the valleys is small (about 0.86 mm); mesial and distal cingula are present and extend along the vestibular side of the tooth (Pandolfi, 2013). The vestibular groove is deep. MPUR 1412-8

Table 6
Morphometric comparisons between the third metacarpal from Vitinia gravels and sands and *S. etruscus*, *S. hundsheimensis*, *S. hemitoechus* and *S. kirchbergensis*.

MCIII	Specimen	Lmax	PTD	PAPD	TDS	APDS	DTD	DAPD	DTDa
Vitinia	MPUR 9/3 ex2768	196	51	46.2	45.3	19	55	42	47.7
S. etruscus	min–max	192–220.5	48.5–58	42–51	45–53.5	18–24.5	49–61	35–43	43–50
S. hundsheimensis	min–max	188.5–221	51–63	42–51.5	46–58	18.5–24	52.5–65.5	39–46.5	43–54.5
S. hemitoechus	min–max	175–203	53.5–65	42.5–57	42.5–57	19–26.5	52–66	43–50.5	48.5–56
S. kirchbergensis	min–max	206–250.5	58–71	50–59	54–70.5	22–26.5	64.5–83	48–58.5	52–64.5

Data from Guérin, 1980.
All dimensions are in mm. Lmax: maximal length; PTD: proximal transverse diameter; PAPD: proximal antero-posterior diameter; TDS: transverse diameter of the shaft; APDS: antero-posterior diameter of the shaft; DTD: distal transverse diameter; DAPD: distal antero-posterior diameter; DTDa: transverse diameter of the distal articular surface.

Table 7
Morphometric comparisons between the femur from Ponte Molle gravels and sands and *S. etruscus*, *S. hundsheimensis*, *S. hemitoechus* and *S. kirchbergensis*.

Femur	Specimen	TDa	APDa	PTDmax	H3th	TD3th
Ponte Molle	MPUR 1523-2	77	70	169	64	127
S. etruscus	min–max	68–89	66–83	145–187	42–76	101–140.5
S. hundsheimensis	min–max	74–95	72–88	158–186	49–76.5	107–142
S. hemitoechus	min–max	83–101	80.5–94	180–211	58.5–90	123–163
S. kirchbergensis	min–max	90–103	85–96.5	193–221.5	67–96.5	142–161.5

Data from Guérin, 1980.
All dimensions are in mm. TDa: transverse diameter of the articular head; APDa: antero-posterior diameter of the articular head; PTDmax: transverse diameter of the proximal epiphysis; H3th: height of the third trochanter; TD3th: transverse diameter at the level of the third trochanter.

differs from *S. kirchbergensis*, which displays a U-shaped anterior lingual valley, a strong difference in height between the bottoms of the lingual valleys and lacks of mesial and distal cingula (Lacombat, 2006). The morphological differences between the studied specimen and *S. hundsheimensis* and *S. hemitoechus* are relatively few. In the considered sample of *S. hemitoechus*, the labial cingulum is absent on the talonid whereas it is present on the m1 of *S. hundsheimensis* from Sussenborn (IQW).

A small-sized femur (MPUR 1523-2: Fig. 3(C, D)) lacks the distal epiphysis whereas the third trochanter is intact and well-evident (Pandolfi, 2013). The proximal articular head is more developed transversally than the trochanter. The femur is dimensionally close to *S. etruscus* than to *S. hundsheimensis* (Table 7). The proximal articular head is proportionally similar to that of the small-sized *S. hundsheimensis* from Vallonnet (Pandolfi, 2013). In proximal view, MPUR 1523-2 has a more elliptical shape of the articular surface with respect to *S. etruscus* from Pietrafitta and Upper Valdarno, and the trochanter is less massive than in the large-sized *S. hundsheimensis*. This specimen is provisionally referred as *Stephanorhinus* aff. *hundsheimensis*.

4.1.5. Ponte Molle, tufaceous conglomerate levels

Two teeth of *S.* cf. *hemitoechus* (MPUR 1439-134; MPUR 1448-51) and three teeth of *S. kirchbergensis* (MPUR 1417-115; MPUR 1456-126; MPUR 1415-63) were collected from the tufaceous conglomerate levels (Pandolfi, 2013; Tables 4 and 5).

P3 (MPUR 1439-134) is highly worn; the mediofossette is closed, the antecrochet and the cingula are absent. On dp4 (MPUR 1448-51), the lingual valleys have a broad V-shaped morphology, mesial and distal cingula are present and the vestibular groove is deep. The morphometrical characters of these two teeth are close to the minimal values for *S. hemitoechus* (Pandolfi, 2013).

P4 (MPUR 1456-126) is relatively large (Table 4); the crochet is present; a slight lingual cingulum and a mesial one occur. M2 (MPUR 1417-115) displays a paracone constriction and the profile of the ectoloph is rather flat. m3 (MPUR 1415-63) has U-shaped lingual valleys and slight mesial and distal cingula. In addition, the difference in height between the bottoms of the valleys is strong and the vestibular groove is deep. In agreement with Pandolfi (2013), these last three teeth are morphologically close to *S. kirchbergensis*.

4.1.6. Tor di Quinto

An isolated upper deciduous tooth (MPUR 1425-98; Table 4) is rather hypsodont. In occlusal view, the ectoloph profile is wavy, with a long and oblique parastyle, a marked paracone fold, a weak metacone fold and a long metastyle. The protoloph and metaloph are long and rather parallel, the postfossette is wide, and a small subcircular fossette is present at the level of the posterior angle between the metaloph and the ectoloph. Two enamel folds are present on the anterior border of the metaloph; protocone and hypocone are separated. The mesial cingulum is present, and the lingual cingulum is oblique and placed only on the hypocone. The deciduous teeth of the genus *Stephanorhinus* are less hypsodont than the specimen from Tor di Quinto; moreover, the ectoloph profile is generally convex, and the protoloph and metaloph are not too long. The specimen slightly resembles the deciduous of *Coelodonta*, but differs in having a quite parallel protoloph and metaloph and in lacking a mediofossette.

An isolated DP3 (MPUR 1425-99; Fig. 4(C), Table 4) displays a slightly convex profile of the ectoloph with a long parastyle and a weak paracone fold. Shallow folds are present in the median valley; the postfossette is wide, the mesial cingulum is present and the lingual cingulum is weak and reduced. The tooth is low-crowned and does not belong to *C. antiquitatis*. On DP3s of *S. hundsheimensis* and *S. hemitoechus*, the profile of the ectoloph displays a marked paracone fold and the mediofossette is often present. The morphological characters of the tooth suggest an attribution to *S. kirchbergensis*.

The P4 (MPUR 1447-123; Table 4) is damaged on the mesial side; the preserved area of the ectoloph displays a shallow metacone fold. The crochet is double, the crista and the antecrochet are absent, the postfossette is transversally elongated, the metaloph is slightly shorter than the protoloph, and the hypocone is constricted. The reduced lingual cingulum is oblique on the hypocone. The overall morphology of the tooth allows excluding an attribution to *Coelodonta* (which is characterised by hypsodont teeth, wavy ectoloph profile, and protoloph and metaloph lingual-distally directed). Contrary to MPUR 1447-123, *S. hundsheimensis* is usually characterised by a well-developed lingual cingulum on P4. The metacone fold is recognised on P4 of *S. hemitoechus* (in the specimen NHML 45205), whereas in studied sample of *S. kirchbergensis*, this character is not evident. Unfortunately, the preserved characters are not sufficient for a safe taxonomic attribution.

An isolated P3 (MPUR 1457-108; Table 4) displays a large parastyle, a little developed paracone fold and a weak mesostyle. The crista is very small, the crochet is bifurcated, the postfossette is small and transversally elongated, and the protocone and hypocone are separated. The mesial cingulum is present and the lingual cingulum is reduced and oblique on the hypocone. On the studied sample of P3s of *S. hundsheimensis*, the lingual cingulum is continuous and horizontal, and the paracone fold is not evident; nevertheless crista and complex crochet are reported for this species (Lacombat, 2006). P3s of *S. kirchbergensis* are characterised by a subtrapezoidal shape, a larger parastyle, and by the absence of the lingual cingulum on the hypocone. On P3s of *S. hemitoechus*, the metacone fold is sometimes evident, the crochet is usually single and the crista is usually absent. Accordingly, a specific attribution appears inaccurate and we prefer to leave the specimen in open nomenclature.

On the dp3 (MPUR 1424-44; Table 5), the trigonid is angular, the vestibular wall of the trigonid is flat, the vestibular groove is shallow, the anterior lingual valley is V-shaped, and the posterior lingual valley is broad V-shaped. The cingula are absent. The specimen resembles the dp3s of *S. kirchbergensis* from Taubach (MfN). Nevertheless, the lingual valleys of dp3s of *S. kirchbergensis* have a U-shaped morphology and, within the considered material, only one specimen displays a V-shaped anterior lingual valley. The specimen from Tor di Quinto differs from *S. hundsheimensis* and

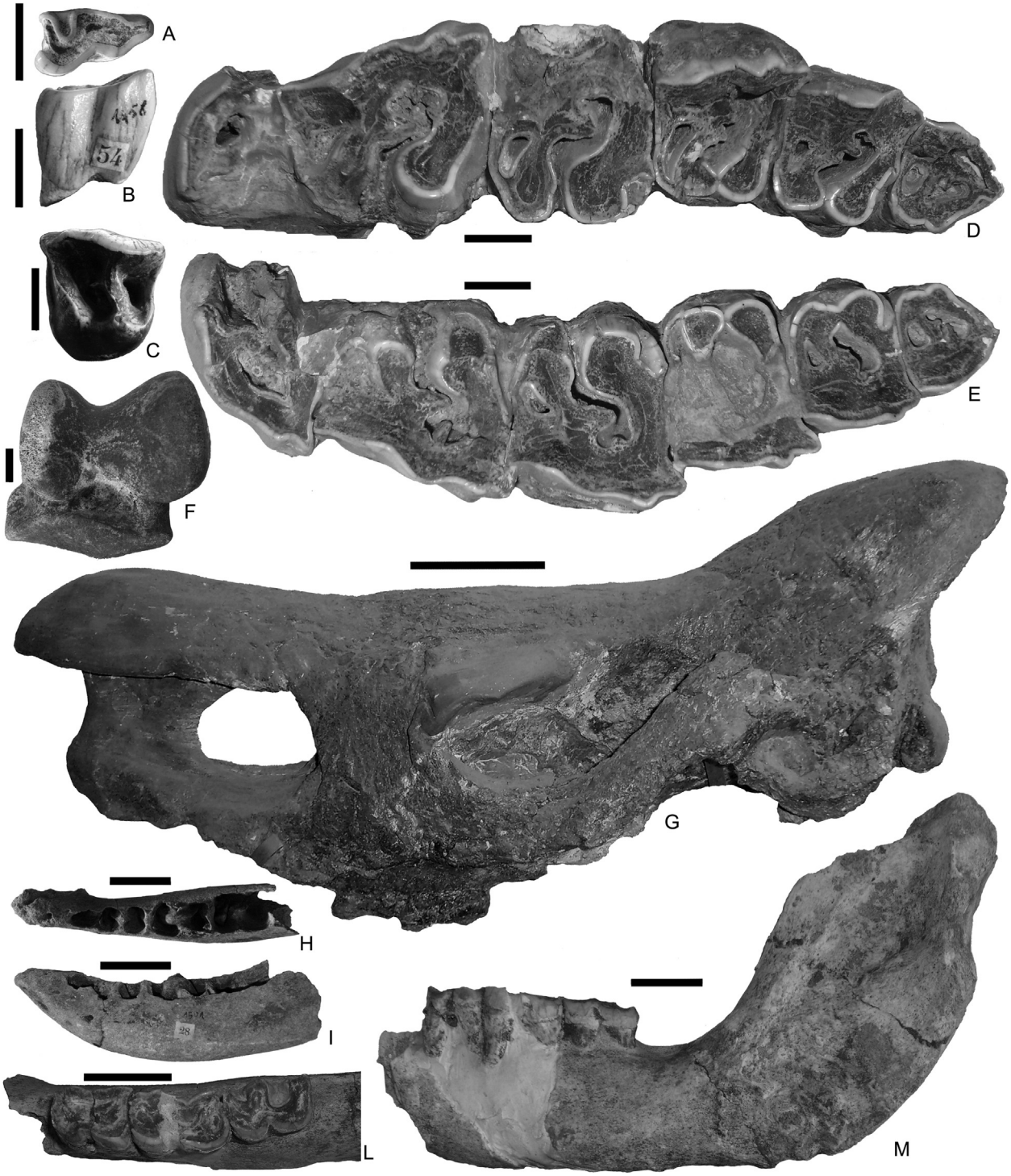

Fig. 4. *Stephanorhinus kirchbergensis* and *S. hemitoechus* from the urban area of Rome. **A**, **B**. p2 (MPUR 1458-54) of *S. kirchbergensis* from Tor di Quinto, in occlusal (A) and labial (B) views. **C**. DP3 (MPUR 1425-99) of *S. kirchbergensis* from Tor di Quinto in occlusal view. **D, E**. Right (D; MPUR 1497) and left (E; MPUR 1497a) upper tooth series of *S. hemitoechus* from Monte Sacro in occlusal view. **F**. Astragalus (MPUR 1510) of *S. hemitoechus* from Monte Sacro in anterior view. **G**. Skull of *S. hemitoechus* (MPUR v2832) from Fosso di Malafede in lateral view. **H**, **I**. Juvenile hemimandible (MPUR 1501-28) of *S.* cf. *hemitoechus* from Vigna San Carlo, in dorsal (H) and labial (I) views. **L**, **M**. Fragmentary hemimandible (MPUR 1514-148) of *S. hemitoechus* from Vigna San Carlo: L, occlusal view of the molars; M, lateral view of the hemimandible. Scale bars: 2 cm (A–F, H–M), 10 cm (G).

S. hemitoechus in which the presence of cingula is usually reported but which are characterised by V-shaped lingual valleys. Based on the compared material, the specimen MPUR 1424-44 is currently referred as *Stephanorhinus* sp.

The p2 (MPUR 1458-54; Fig. 4(A, B), Table 5) displays two lingual valleys; the anterior one is slightly marked, and the posterior one has a narrow V-shape morphology. The paralophid is single and straight, and the paraconid is developed (Fig. 4(A)); the cingula are absent. The presence of the anterior lingual valley is usually recorded only on p2s of *S. kirchbergensis* and *S. hemitoechus* (Guérin, 1980; Lacombat, 2006). Contrary to the considered specimen, p2 of *S. hemitoechus* is transversally wider at the base of the crown and the enamel on the vestibular wall is rougher. An attribution to *S. kirchbergensis* is therefore supported.

Table 8
Morphometric comparisons between the astragalus from Monte Sacro and *S. etruscus*, *S. hundsheimensis*, *S. hemitoechus*, *S. kirchbergensis* and *C. antiquitatis*.

Astragalus	Specimen	TDmax	TDDmax	Hmax	APDm	DTDa	DAPDa
Monte Sacro	MPUR 1510	90	77	88	58	72	46
S. etruscus	min–max	73–88	60–78	71–84	47–58	57–75	36–45.5
S. hundsheimensis	min–max	76–107	61–82	67–89	46–68	59.5–85	35–52
S. hemitoechus	min–max	72.5–95	63.5–82	72–94	48–67	60.5–80	34–55
S. kirchbergensis	min–max	93–113	79–99	85–105	55–83	74–93	42–60
C. antiquitatis	min–max	84–112	75–97	77–102	52–72	68–91	42–79

Data from Guérin, 1980.
All dimensions are in mm. TDmax: maximal transverse diameter; TDDmax: maximal distal transverse diameter; Hmax: maximal height; APDm: medial antero-posterior diameter; DTDa: transverse diameter of the distal articular surface; DAPDa: antero-posterior diameter of the distal articular surface.

p3 (MPUR 1455-87; Table 5) is highly worn; the lingual valleys are not evident and the tooth is covered by cement. The latter character suggests an attribution to *S. hundsheimensis* or *S. hemitoechus* rather than *S. kirchbergensis*; nevertheless, a specific attribution is inaccurate due to the state of conservation.

p4 (MPUR 1455-86; Table 5) has a rounded trigonid; the vestibular groove is marked, the lingual valleys have a V-shaped morphology, the difference in height between the bottoms of the valleys is small (0.81 mm), and a small distal cingulum is present. V-shaped lingual valleys are reported in *S. hundsheimensis* and *S. hemitoechus*. The distal cingulum is absent on *S. hemitoechus* (Lacombat, 2006) whereas the difference in height between the bottoms of the valleys is small in p4s of Middle Pleistocene *S. hundsheimensis* and of *S. hemitoechus* from Caune de l'Arago (Lacombat, 2006). On p4s of *S. kirchbergensis* from Grays and Taubach, the vestibular groove is shallow and the posterior lingual valleys are U-shaped. The studied specimen clearly differs from *S. kirchbergensis* but an attribution to *S. hundsheimensis* rather than *S. hemitoechus* is not fully supported.

4.1.7. Monte Verde

A fragmentary mandible with m1 and m2 (MPUR 1422-61) has been collected at Monte Verde (Table 5). The m1 has a V-shaped posterior valley, a marked distal cingulum and a marked and oblique vestibular cingulum; the difference in height between the bottoms of the valleys is small. A weak cingulum occurs below the bottom of the posterior valley.

The m2 has a V-shaped posterior valley and a U-shaped anterior valley; a cingulum occurs below the bottom of the posterior valley. Distal and vestibular cingula are present. The difference in height between the bottoms of the valleys is relatively small. The teeth differ from those of *S. kirchbergensis* (BSPG, IGF, MfN, NHML, SMNK, SMNS), which display a smooth enamel and especially U-shaped lingual valleys. The morphological characters of the specimen from Monte Verde resemble those of *S. hundsheimensis* and *S. hemitoechus*. The presence of a lingual cingulum below the lingual valley has never been reported for *S. hundsheimensis* and suggests an attribution to *S. hemitoechus* (Guérin, 1980; Lacombat, 2005). Nevertheless, lingual cingula occur below the lingual valley of the molars of *S. hundheimensis* from Hundsheim (NHMW). A specific attribution of the specimen from Monte Verde is therefore inaccurate.

4.1.8. Sedia del Diavolo

From the clay layer of Sedia del Diavolo, a second metacarpal has been found (Caloi et al., 1980). At present, this remain is not available because it was not found in the collections. However, according to Caloi et al. (1980), it has dimensional characters similar to *S. kirchbergensis* but they ascribed it to an indeterminate species. The specimen is referred here as *Stephanorhinus* sp., waiting the opportunity to observe directly its morphology.

From the upper gravels of Sedia del Diavolo, a highly worn P2, a fragment of P2 and a m1 have been found (Caloi et al., 1980). The P2s seem not available and the dimensions of one of them are not useful for an accurate taxonomic attribution (Caloi et al., 1980). The m1 was ascribed to *Dicerorhinus* sp. by Caloi et al. (1980) and later referred to *Dicerorhinus hemitoechus* by Fortelius (1981) and *S. kirchbergensis* by Billia and Petronio (2009). The tooth (Caloi et al., 1980: tav. I, fig. 9) displays V-shape lingual valleys and a deep and marked vestibular groove. These features are not common in *S. kirchbergensis* (Lacombat, 2006). According to Billia and Petronio (2009), the tooth is characterised by thickened and smooth enamel but they did not figure the tooth and these characters cannot be observed on the picture of Caloi et al. (1980). Therefore, in agreement with Fortelius (1981) this specimen, which is not currently present within the MPUR collections, is referred as *S. hemitoechus*.

4.1.9. Monte Sacro, tufaceous conglomerates

The specimens collected at Monte Sacro consist of two maxillae (MPUR 1497 and 1497a), one M2 (MPUR 1426-106), three M3 (MPUR 1427-31, MPUR 1428-24, and MPUR 1478-91), one astragalus (MPUR 1510) (Tables 4 and 8).

The maxillae (MPUR 1497 and 1497a; Fig. 4(D, E), Table 4) are in a good state of preservation and probably belong to the same individual. The cheek teeth are subhypsodont, the enamel is rough and partially covered by cement. On specimen MPUR 1497 (Fig. 4(C)), P2 is relatively small, the ectoloph profile is convex, the crista is present, the crochet is small, the antecrochet is absent, and the protocone is less developed than the hypocone. The postfossette is relatively large and subelliptical, the lingual cingulum is reduced and the mesial cingulum is present. On P3 the ectoloph profile is slightly convex with a developed paracone fold, the crista and antecrochet are absent, the crochet is reduced, the postfossette is small and the lingual cingulum is strongly reduced. The paracone fold is marked on P4, and a shallow metacone fold can be also observed. The parastyle is long, the protocone and hypocone are separated, the mesial and distal cingula are present and the lingual cingulum is strongly reduced. M1 has a developed paracone fold, a small crista, a single crochet, a small postfossette and a constricted protocone. The lingual cingulum is absent. The paracone fold is also developed on M2 and a mesostyle can be observed on this tooth. The posterior profile of the ectoloph is concave, the crista is slightly more developed than on M1, the crochet is single, the metaloph is short and continuous and the postfossette is wide. M3 has a subtriangular shape, the paracone fold is developed, the profile of the ectometaloph is convex and the mediofossette is present. The teeth of the specimen MPUR 1497a (Fig. 4(D)) are quite similar to those of the specimen MPUR 1497 with the following exception: the lingual cingulum is completely absent on the premolars, P4 and P3 display two small crochet and the crista is absent on M2.

The two upper cheek tooth series differ from *S. kirchbergensis* in which the teeth are characterised by bulbously lingual cones, smooth enamel without cement and shallow folds and styli on the ectoloph. In *S. hundsheimensis*, P2 is proportionally larger, the profile of the ectoloph on P3 and P4 is straight with a less developed paracone fold, the lingual cingulum on the premolars is

marked and continuous, the ectoloph on M2 is shorter and the mesostyle is not well-evident; on M3 the mediofossette is usually absent. The morphology of the specimens from Monte Sacro is similar to that of several upper teeth of *S. hemitoechus* collected in a large number of Western European localities.

The isolated M2 (MPUR 1426-106) has a well-developed single crochet, a lingual pillar at the entrance of the medisinus, and a mesial cingulum. The protocone is not constricted and the metaloph is short. The ectoloph profile has a marked paracone fold, a well-evident mesostyle and a concave posterior border. The specimen shares several characters with the M2 of the two maxillae from Monte Sacro and can be ascribed to the same species.

On the isolated M3 (MPUR 1427-31), the paracone fold is developed and the ectometaloph is convex. The mediofossette is present, the mesial cingulum is continuous and a pillar occurs at the entrance of the medisinus. The lingual cones are not bulbously inflated and the enamel is quite rough, contrary to *S. kirchbergensis*. Nevertheless, the morphology of the tooth resembles both *S. hundsheimensis* and *S. hemitoechus*. The presence of a mediofossette could suggest an attribution to *S. hemitoechus*, but this character is also reported in *S. hundsheimensis* (Lacombat, 2006).

M3 (MPUR 1428-24) is much worn and large; the mediofossette is closed and the parastyle is little developed. The protocone is very large and the enamel appears smooth. On M3s of *S. hundsheimensis* and *S. hemitoechus* the protocone is less developed than in the specimen 1428-24 from Monte Sacro and the paracone fold is more developed. An attribution to *S. kirchbergensis* could be supported by the morphology of the paracone fold and the dimensions of the protocone; nevertheless, the specimen is much worn and these characters may be accentuated by the high degree of deterioration of the specimen.

An isolated M3 (MPUR 1478-91) displays a shallow paracone fold, a slightly convex profile of the ectometaloph, a constricted protocone, a double crista, a developed crochet which is placed more lingually than in several Pleistocene rhinoceroses, and a marked lingual groove on the hypocone. The morphology of this tooth has never been observed in the Pleistocene species; it is tentatively referred to *Stephanorhinus* sp.

The astragalus (MPUR 1510; Fig. 4(F), Table 8) displays, in anterior view, a rather symmetric trochlea. The medial lip of the trochlea is less transversally developed than the lateral one; the distal border of the trochlea is delimited by a marked depression. The medial tuberosity is relatively high, with a straight medial border. In posterior view, the proximal articular surface for the calcaneus is much concave and does not extend distally, and the articular surface on the middle of the posterior face is large and subelliptical in shape. In distal view, the articular surface for the navicular is subrectangular in shape, with a convex medial border and a straight anterior border; the articular surface for the cuboid is relatively wide and slightly more forward than that for the navicular. In medial view, the proximal border of the medial lip of the trochlea is regularly convex and the medial tuberosity is placed in the middle of the distal half of the medial face.

The astragalus from Monte Sacro differs from those of *S. hundsheimensis* (MfN, NHML, NHMW) in which the medial border of the medial face, in anterior view, is slightly oblique, the trochlea is slightly asymmetric, and a rounded medial tuberosity extends medially. In the astragalus of *S. kirchbergensis* (MfN, NHML) the trochlea is strongly asymmetric and the medial lip is oblique with respect to the distal border of the bone; the articular surface for the cuboid is long. In *C. antiquitatis* (MfN, NHML, NHMW, NMB) the medial tuberosity is located posteriorly on the medial face, the trochlea is transversally elongated, with the lateral lip more developed than the medial one, and the anterior border of the articular surface for the cuboid extends more forward than that for the navicular. The astragalus from Monte Sacro shares several characters (morphology of the trochlea, morphology of the medial tuberosity) with specimens referred to *S. hemitoechus* housed at NHML, MNCN, MNPELP.

To sum up, the material from Monte Sacro is recognized as *S. hemitoechus*, excepted three M3 (MPUR 1427-31, MPUR 1428-24, and MPUR 1478-91) that are referred to *Stephanorhinus* sp.

4.1.10. Prati Fiscali

Only a strongly worn M3 (MPUR 1476-105) and a strongly worn upper premolar (MPUR 1471) have been collected at Prati Fiscali.

The upper premolar displays a rough enamel covered by cement, a rather straight profile of the ectoloph, and a subcircular postfossette; other characters cannot be observed. The specimen differs from *S. kirchbergensis* by having cement on the enamel, but an attribution to *S. hundsheimensis* rather than to *S. hemitoechus* is not possible.

The lingual cones of M3 are damaged, the roots are not preserved and the mediofossette is present together with a small enamel fold. According to Billia and Petronio (2009), this specimen was collected at Monte Sacro and was ascribed to *S. kirchbergensis*; nevertheless the morphological characters reported by these authors cannot be observed on the considered specimen and a specimen misidentification appears probable. Due to the conservation status of this specimen, a specific attribution is inaccurate.

4.1.11. Batteria Nomentana

The m3 (MPUR 1477-68; Table 5) has a weak vestibular cingulum, a shallow vestibular groove, which does not reach the base of the crown, and a distal and mesial cingulum. The lingual valleys are V-shaped and the difference in height between the bottoms of the valley is small. In *S. kirchbergensis* the lingual valley is usually U-shaped, the vestibular groove is deep, and the difference in height between the bottoms of the valleys is strong (Lacombat, 2006). In *S. hundsheimensis* the vestibular cingulum has been never observed (Lacombat, 2006) but on the anterior loph of the specimens from Hundsheim a vestibular cingulum is present. Moreover, the morphology of the tooth also resembles *S. hemitoechus* and the specimen is therefore ascribed to *Stephanorhinus* sp.

4.1.12. Vigne Torte

Several fragmentary teeth have been collected at Vigne Torte. A damaged M2 (MPUR 1489-111) displays an incipient mesostyle, a single crochet, a double crista and a single antecrochet. The enamel appears smooth but the specimen is rather polished. The antecrochet and the double crista are absent on the studied M2s of *S. kirchbergensis* (mostly represented by the specimens from Grays and Taubach). A small antecrochet is present on M2s of *S. hundsheimensis* from Voigsted (IQW) but is absent in those from Hundsheim (NHMW) and Sussenborn (IQW); the latter specimens also lack of double or multiple crista. Antecrochet and double or multiple crista are evident on some M2s of *S. hemitoechus* from Grays and Ilford (NHML). Consequently, the specimen MPUR 1498-111 is referred to *S. hemitoechus*.

A much worn M1 (MPUR 1469-93) does not display useful morphological characters for a safe taxonomic attribution. A fragment of an unworn lower premolar (MPUR 1470-76) displays a V-shaped posterior lingual valley and a convex vestibular profile of the talonid. The specimen is poorly preserved for a specific taxonomic attribution. A fragmentary lower molar (MPUR 1474-48) has an opened vestibular groove, a broad V-shaped posterior lingual valley and a small difference in height between the bottoms of the lingual valleys. The enamel is relatively rough. The specimen differs from *S. kirchbergensis* in the morphology of the posterior

valley and in the character of the enamel but it cannot be confidently referred to *S. hundsheimensis* or *S. hemitoechus*.

4.1.13. Vigna San Carlo

A fragmentary mandible without teeth (MPUR 1501-28) of a young and a fragmentary mandible with molars (MPUR 1514-148) of an adult individual were discovered at Vigna San Carlo (Tables 3 and 5).

The juvenile mandible (MPUR 1501-28; Fig. 4(H, I)) lacks the vertical ramus. The ventral border of the mandible is regularly convex, the maximal width of the horizontal ramus is at the level of the alveolus of dp4 and a small mental foramen occurs at the dp1-dp2 boundary. A small rounded alveolus for dp1 occurs in front of dp2. The specimen differs from the juvenile mandible of *S. kirchbergensis* from Taubach, which is characterised by a rather constant height of the horizontal ramus and a less convex lower border of the mandible in lingual view. A juvenile mandible of *S. hundsheimensis* from Mosbach displays a less convex ventral border in lingual view than in the studied specimen; the mental foramen is located below dp1. Morphologically, the specimen from Vigna San Carlo resembles a juvenile mandible of *S. hemitoechus* from San Sidero (Late Pleistocene, Apulia; MPM), but the comparison material is too poor for a safe taxonomic attribution.

The mandible MPUR 1514-148 (Fig. 4(L, M)) is represented by the vertical ramus and by the molar portion of the horizontal one. The vertical ramus is massive and the angle with the horizontal ramus is obtuse. The preserved lower border of the mandible is rather straight. The molars are much worn and a few morphological characters can be observed. The enamel is rough and the cement is present; a lingual cingulum occurs below the posterior valley on M3 and the difference in height between the bottoms of the valleys on M3 is small. All these characters are present on the mandibles of *S. hemitoechus* from Val di Chiana (NMB) and Ilford (NHML). The specimen differs from *S. kirchbergensis* in which the lingual valleys are usually U-shaped, the angle between the horizontal and vertical rami is of about 90°, the lower border of the horizontal ramus is more convex, and the enamel of the teeth is generally smooth. In *S. hundsheimensis* the vertical ramus has a less oblique anterior border, the distance between the vertical ramus and the posterior border of M3 is short, the posterior border of the mandible is more convex than in the specimen from Vigna San Carlo, and the lingual cingulum is generally absent on the molars but it can be observed on the specimen from Hundsheim. The adult mandible from Vigna San Carlo is therefore assigned to *S. hemitoechus*.

4.1.14. Vitinia, upper levels, and Fosso Malafede

The localities of Vitinia (upper levels) and Fosso Malafede are very close to each other and are characterised by the same sedimentary deposit.

The skull from the upper levels of Vitinia (MPUR v2766; Table 1) was ascribed to *Dicerorhinus hemitoechus* by Caloi et al. (1981). The specimen is relatively damaged in the occipital region; however, the occipital crest seems to extend posteriorly and the occipital face, in lateral view, is straight. The external auditory pseudomeatus is ventrally closed. In occipital view, the occipital face is trapezoidal and the maximal width is at the level of the mastoid processes. The dorsal profile of the occipital crest is straight. The morphology of the fragmentary skull from Vitinia differs from that of *S. kirchbergensis* in which the occipital condyles are more extended posteriorly than the occipital crest and the latter is less transversally developed. The specimen shares a few features with the skull of *S. hundsheimensis* from Hundsheim and the differences are in the morphology of the occipital crest, in the presence of a slightly more developed nuchal tubercle and in a less high occipital face. The studied specimen shares several features with the skulls of *S. hemitoechus* from some Middle Pleistocene localities (Clacton, Campagna Romana). In these specimens, as well as in that from Vitinia, the nuchal tubercle is little developed, the occipital face is straight and the occipital crest is less posteriorly extended and less transversally developed than in the skulls of *S. hemitoechus* from Ilford and Ponte alla Nave. The specimen from Vitinia is here referred to *S. hemitoechus*.

The skull from Fosso di Malafede (MPUR v2832; Fig. 4(G), Table 1) displays a well-developed occipital crest, in lateral view, which overhangs the occipital condyles. The dorsal profile of the skull is concave, the anterior border of the orbital cavity is at the M2-M3 boundary and the external auditory pseudomeatus is ventrally closed. The posterior border of the occipital crest is straight in dorsal view. In occipital view, the occipital face is subtrapezoidal, the dorsal profile of the occipital crest is straight and the foramen magnum is subcircular with a dorsal incision. The morphology of the skull is similar to that of *S. hemitoechus* from Campagna Romana (Pandolfi et al., 2013a).

4.1.15. Rome, Tiber River terraces, undefined locality

An unpublished isolated (first?) lower molar (MGGC 33), a third(?) upper deciduous (MGGC 33), and a neurocranial portion of a fragmentary skull (MGGC nn) were collected from an undefined deposit of the Tiber River within or near the city of Rome.

In dorsal view, the fragmentary skull (Fig. 5(A–C), Table 1) displays a straight posterior border of the occipital crest and distant frontal-parietal crests (Fig. 5(A)). In lateral view, the frontal-parietal crests are well-evident, the external auditory pseudomeatus is closed, the occipital crest overhangs the occipital condyles and the occipital face is straight (Fig. 5(B)). In occipital view, the dorsal border of the occipital crest is convex, the occipital face is bell-shaped, and the foramen magnum is subtriangular in shape (Fig. 5(C)). The overall morphology of the fragmentary skull is close to that of *Coelodonta antiquitatis* from several European localities (HNHM, MfN, NHML, NHMW, NMB). The specimen differs from *S. hemitoechus*, which has a subtrapezoidal shape of the occipital face and a less developed occipital crest. In *S. hundsheimensis* and *S. kirchbergensis*, the occipital crest does not overhang the occipital condyles; in *S. kirchbergensis*, the occipital face is subtrapezoidal in shape whereas in *S. hundsheimensis*, the dorsal profile of the parietal is less inclined.

The lower molar is hypsodont (Fig. 5(E, F)), the anterior lingual valley is V-shaped, the posterior lingual valley is broad V-shaped, the trigonid is angular, the hypolophid is almost sagittal and the vestibular wall of the lophs is flat. The tooth clearly differs from those of the species of the genus *Stephanorhinus* whereas it is morphologically similar to those of the genus *Coelodonta*.

The upper deciduous (Fig. 5(D)) has a wavy ectoloph, and a long and curved parastyle and metastyle; the metaloph is backwards, the postfossette is wide and the lingual cingulum is absent. The median valley is filled by sediment and the presence of a mediofossette is not evident. The specimen morphologically resembles the DP2s/DP3s of *Coelodonta antiquitatis*. An attribution to the genus *Stephanorhinus* can be excluded based on the hypsodonty of the tooth, the obliquity of the metaloph and the wave of the ectoloph.

4.1.16. Rome, urban area, undefined locality

Four upper cheek tooth series (MPUR 1498, MPUR 1499, MPUR 1518, MPUR 1519; Fig. 6) were collected somewhere in the urban area of Rome (Suburb area when collected).

On specimen MPUR 1498 (Fig. 6(A)), P2 displays a mesial and lingual cingulum, the protocone less developed than the hypocone, a rounded postfossette and several small enamel folds on the posterior border of the median valley. P3 has a long parastyle, the ectoloph is slightly convex with a shallow paracone fold and a very

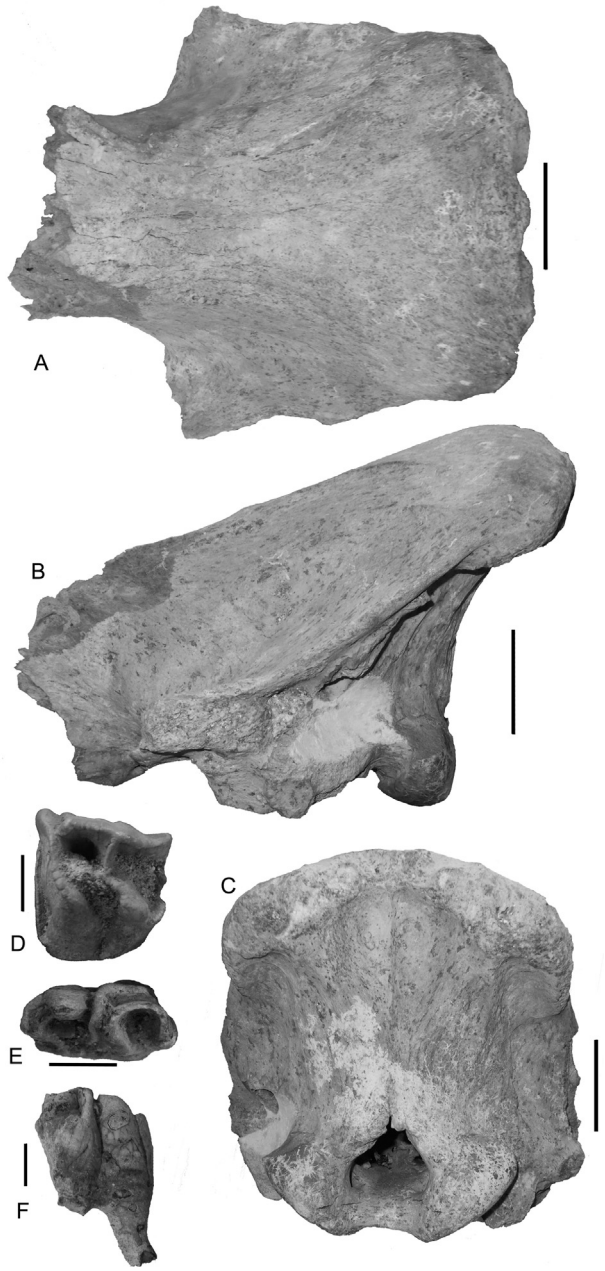

Fig. 5. *Coelodonta antiquitatis* from the Tiber River terraces. **A**–**C**. Fragmentary skull (MGGC nn), in dorsal (A), lateral (B) and occipital face (C) views. **D**. Upper deciduous (MGGC 33) in occlusal view. **E**, **F**. Lower molar (MGGC 33), in occlusal (E) and labial (F) views. Scale bars: 5 cm (A–C), 2 cm (D–F).

shallow metacone fold, the crochet is double, the crista and antecrochet are absent, the postfossette is small and circular, the protocone and the hypocone are separated and the lingual cingulum is present on the hypocone. P4 has a wavy ectoloph with a shallow paracone fold and a weak mesostyle, the crochet is multiple, the antecrochet is absent, the protoloph and metaloph are continuous, the protocone and hypocone are separated, and the lingual cingulum is continuous, oblique and joined with the mesial and distal cingulum. M1 is much damaged, the mesostyle is weak, the crista is present, the crochet is single, the antecrochet is absent, the postfossette is rounded and the metaloph is continuous. M2 has a shallow paracone fold and a concave posterior border of the ectoloph, the crista is present, the crochet is single and the antecrochet is represented by a shallow and small enamel fold; the metaloph is short, the postfossette is wide, the protocone is slightly constricted and the lingual cingulum is absent. M3 is small, subtriangular in shape, with a convex ectometaloph and a shallow paracone fold, the mediofossette is present, the protocone is not constricted, the lingual cingulum is absent and the lingual cones are not bulbously inflated.

On specimen MPUR 1499, P3 has a very shallow paracone fold, a single crochet and a protocone constriction. P4 has a rather straight profile of the ectoloph, the crochet is small, the lingual cingulum is absent and the postfossette is small. M1 has an evident paracone fold, a weak mesostyle, a concave posterior profile of the ectoloph, a weak crochet and a protocone constriction. On M2, the paracone fold is shallow, the mesostyle is not evident, the posterior border of the ectoloph is concave, the crochet is single, the metaloph is short and continuous and the lingual cingulum is absent. The paracone fold is also shallow on M3, where the crochet is well-developed and bifurcated, the lingual cingulum is absent, and the protocone constriction is absent.

On specimen MPUR 1518 (Fig. 6(B)), P2 is subtrapezoidal, the ectoloph profile of this tooth is slightly convex, the paracone fold is not evident, the crista and the antecrochet are absent, the crochet is small, the postfossette is transversally elongated, the protocone is less developed than the hypocone, and the lingual cingulum is absent. The ectoloph profile on P3 does not display evident folds, the crista and the antecrochet are absent as well as the crochet, the postfossette is transversally elongated, the mesial cingulum is present and the lingual cingulum is weak. P4 has a shallow paracone fold and a generally convex profile of the ectoloph; the crista is present, the crochet is single, the protocone and the hypocone are separated and the lingual cingulum is absent. M1 has a slightly convex posterior profile of the ectoloph; the crochet is single, the crista and the antecrochet are absent, the metaloph is short, the protocone is weakly constricted and the lingual cingulum is absent. M2 is damaged and the only useful morphological character observable is a shallow paracone fold. M3 has a shallow paracone fold, a regularly convex profile of the ectometaloph, and a single crochet.

On specimen MPUR 1519 (Fig. 6(C)), P3 has a slightly convex profile of the ectoloph, the paracone fold is absent, the mesial cingulum is present, the lingual cingulum is absent and the hypocone is constricted. P4 has a long parastyle, a shallow paracone fold, a relatively long metastyle and a mesial cingulum, whereas the lingual cingulum is absent. M1 is strongly damaged, the antecrochet is absent and the protocone is weakly constricted. The ectoloph on M2 has a shallow paracone fold, a very weak mesostyle and a concave posterior profile. M3 is subtriangular in shape, relatively small and with a shallow paracone fold.

According to Billia and Petronio (2009), all these specimens can be referred to *S. kirchbergensis* and the specimens MPUR 1518 and MPUR 1519 belong to the same individual. Nevertheless, the observation of the specimens by one of us (L.P.) shows that the specimens MPUR 1498 and MPUR 1499 are probably a composition of different teeth of different individuals collected separately.

On the specimen MPUR 1498 (Fig. 6(A)), P2, M1 and M3 are much worn, whereas P4 and M2 are moderately worn. The stages of wear of the teeth are not in agreement with the tooth eruption sequence reported for the extant rhinoceroses (Goddard, 1970; Hillman-Smith et al., 1986; Koenigswald et al., 2007; Pandolfi, pers. observ.). Actually, in all rhinoceroses and most mammals (ungulates at least), the M1 is the first erupting molar. In recent rhinoceroses, M3 is the last one; therefore, M3 and M1 cannot present similar stages of wear. Moreover, P4 erupts before M3 in recent rhinoceroses, and it should be more worn than M3. In addition, M3 is filled by a volcaniclastic sediment which is not present on the other teeth; on this tooth, the roots are also brown and covered by sediment whereas the roots of the other teeth are black and without sediment. On the specimen MPUR 1499, P3-M1

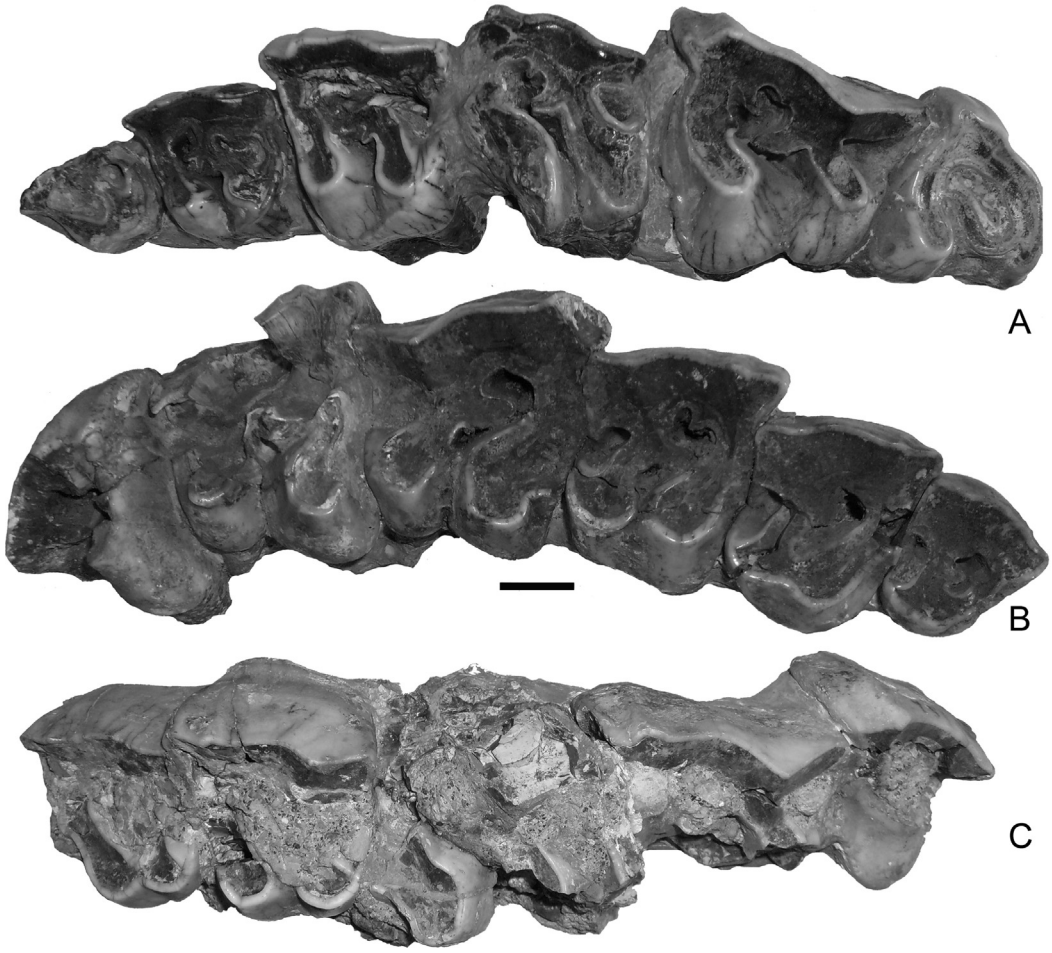

Fig. 6. Upper tooth rows of *Stephanorhinus kirchbergensis* from the urban area of Rome. **A**. P2-M3 (MPUR 1498) in occlusal view, but only P3-P4 and M2 are referred as *S. kirchbergensis*. **B**. P2-M3 (MPUR 1518) in occlusal view. **C**. P3-M3 (MPUR 1519) in occlusal view. Scale bar: 2 cm.

is highly worn and has a similar stage of wear, whereas M2 (which erupts together or before P4) is moderately worn. Moreover, P3-M1 and M2-M3 have a different state of conservation. Based on these observations, the teeth in both specimens probably belong to different individuals and they need to be compared separately.

P3 and P4 of the specimen MPUR 1498 can be ascribed to *S. kirchbergensis* and differ from *S. hundsheimensis* and *S. hemitoechus*, which display a more developed paracone fold, a less wavy profile, and cement and roughness on the enamel. The presence of bulbous lingual cones and the shallow paracone fold suggest an attribution to *S. kirchbergensis* also for the M2. P2 and M1 cannot be ascribed to a well-defined species due to the state of conservation.

In *S. hemitoechus*, the paracone fold is more marked on M3 and the tooth is larger than in the M3 of the specimen MPUR 1498; the latter is morphologically close to the specimens of *S. hundsheimensis* from Hundsheim (NHMW). Nevertheless, in *S. hundsheimensis*, the mediofossette is rarely present. A specific attribution of the M3 of the specimen MPUR 1498 is currently excluded.

P3-M1 of the specimen MPUR 1499 are not ascribed to a well-defined species because the teeth are highly worn and useful morphological characters cannot be observed. M2 of the specimen MPUR 1499 is morphologically very similar to that of the specimen MPUR 1498 and to the M2 from Kirchberg (NMB); accordingly, it can be ascribed to *S. kirchbergensis*. The M3 of MPUR 1499 is larger than that of the specimen MPUR 1498 and displays a shallow paracone fold and a slightly bulbous protocone. These characters are evident on M3 of *S. kirchbergensis* from Kirchberg (NMB).

The stages of wear of the teeth on the specimens MPUR 1518 and MPUR 1519 are rather similar and they could actually belong to the same individual. The profile of the ectometaloph on M3 and of the ectoloph on M2 (which are very similar to those of the specimens from Kirchberg) and the morphology of the premolars suggest an attribution to *S. kirchbergensis*.

4.2. Rhinocerotidae-bearing localities of the urban area of Rome: chronology and stratigraphy

4.2.1. Monte delle Piche

The Monte delle Piche Series was introduced by Conato et al. (1980) at the homonymous type locality, who distinguished it from the older Monte Mario Formation (Bonadonna, 1968) based on the presence of *Hyalinea baltica*. It is tentatively correlated with MIS 21 (ca. 0.85 Ma; Lisiecki and Raymo, 2005) based on its stratigraphic relationship with respect to the younger deposits of the PG1 Formation (Karner et al., 2001a), which in turn are linked to MIS 19 by paleomagnetic and geochronologic constraints (Marra and Florindo, 2014). A lower age boundary at 1.59 Ma for the Monte delle Piche deposits is inferred based on attribution of the underlying Monte Mario Formation to MIS 57-55 (Cosentino et al., 2009).

The rhinoceros remains from Monte delle Piche locality were embedded in marine clay sediments, as evidenced by the micropaleontological study on a fraction of this clay (Pandolfi et al., 2013b, 2015), showing the presence of *Neogloboquadrina*

pachyderma (sinistral coiling; Pandolfi et al., 2015) and indicating an age younger than the Gelasian. However, the abovementioned literature data allow to confidentially constraining the age of the Monte delle Piche Formation, and of the embedded fossils, to the interval 1.6–0.8 Ma. Moreover, litostratigraphic, biostratigraphic and paleogeographic considerations (Marra and Florindo, 2014) strongly suggests that the clay sediments at Monte delle Piche were deposited during the highstand of MIS 21 (858–821 ka; Bassinot et al., 1994), immediately preceding the glacio-eustatic cycle linked to MIS 20-19, during which the overlying deposits of the PG1 Formation were deposited.

4.2.2. Cava Redicicoli

The fossiliferous site of Cava Redicicoli has been interpreted to host sediments of the Paleo-Tiber 2, 3 and 4 aggradational successions (Marra et al., 2014a), based on the reconstruction of the stratigraphic setting of this area performed by means of boreholes data in Marra and Florindo (2014). However, the gravel layers from which the fossil remains are reported to come (Blanc, 1955) are correlated to those occurring few kms south of Rome. Age of this gravel is tightly constrained by those of several tephra layers spanning 806 ± 6–788 ± 9 ka (Florindo et al., 2007), providing correlation with the Paleo-Tiber 2 Formation and with MIS 20-19 (Marra and Florindo, 2014).

4.2.3. Vitinia, gravels and sands

The gravel layer cropping out at the base of type-section of the Vitinia Formation in the homonymous locality described in Conato et al. (1980) has been attributed to the Paleo-Tiber 4 aggradational succession (Marra and Florindo, 2014) of the Santa Cecilia Formation, which correlates to MIS 16-15 (Karner and Marra, 1998). A $^{40}Ar/^{39}Ar$ age of 653 ± 4 ka (Karner et al., 2001b) is provided for a pyroclastic-flow deposit at the top of the gravel layer of the Paleo-Tiber 4 aggradational succession at the INGV borehole, ca. 8 km northeast of Vitinia (Marra and Florindo, 2014). However, based on correlation with the Oxygen isotopes timescale, deposition of the gravel layer of the Paleo-Tiber 4 aggradational cycle is supposed to last until the MIS 16-15 transition, at 621 ka (Lisiecki and Raymo, 2005). Therefore, we assess an age spanning 0.65–0.62 Ma to the fossil remains collected at Vitinia locality.

4.2.4. Ponte Molle (= Ponte Milvio)

The stratigraphic setting of the sector comprising the foothill of Monte Mario and the Tiber Valley, where the Mulvian Bridge (Ponte Milvio) is located, is reconstructed in Marra et al. (1995) by means of borehole stratigraphies and field data. Here we have re-interpreted the cross-section given by Marra et al. (1995: fig. 10) in the light of the most recent acquisitions on the chronostratigraphy and paleogeography of Rome (Marra and Florindo, 2014; Fig. 7).

4.2.4.1. Gravels and sands levels. The lowest gravel layer (noted "a" in Fig. 7) correlates well, based on its lateral extension and elevation, with the widespread basal gravel of the Paleo-Tiber 2 cycle, which is present below the younger volcanic cover in the northern area of Rome (Marra and Florindo, 2014). As provided for the coeval Cava Redicicoli gravels, we assign an age of 0.81–0.79 Ma to this horizon.

4.2.4.2. Tufaceous conglomerate levels. The uppermost gravel layer occurring in the west portion of the cross-section (noted "b" in Fig. 7) correlates with a similar gravel layer cropping out around 40 m a.s.l. in Via Flaminia Nuova, 1.5 km to the north, on top of which a tephra layer dated at 465 ± 7 ka occurs (Karner and Renne, 1998). Age of this tephra represents the lower age boundary provided by the aggradational succession of the San Paolo Formation to glacial termination V, at the MIS 12-11 transition (Karner and Marra, 1998). However, after considering the possible reworking of this tephra, also in the light of the better constraints with the Oxygen isotopes timescale provided by a younger tephra layer occurring above the gravel within the deposit of the San Paolo Formation dated at 427 ± 5 ka (Karner and Renne, 1998; Marra et al., 2014b), a timespan of 0.46–0.43 m.y. is assumed here for the deposition of the gravel

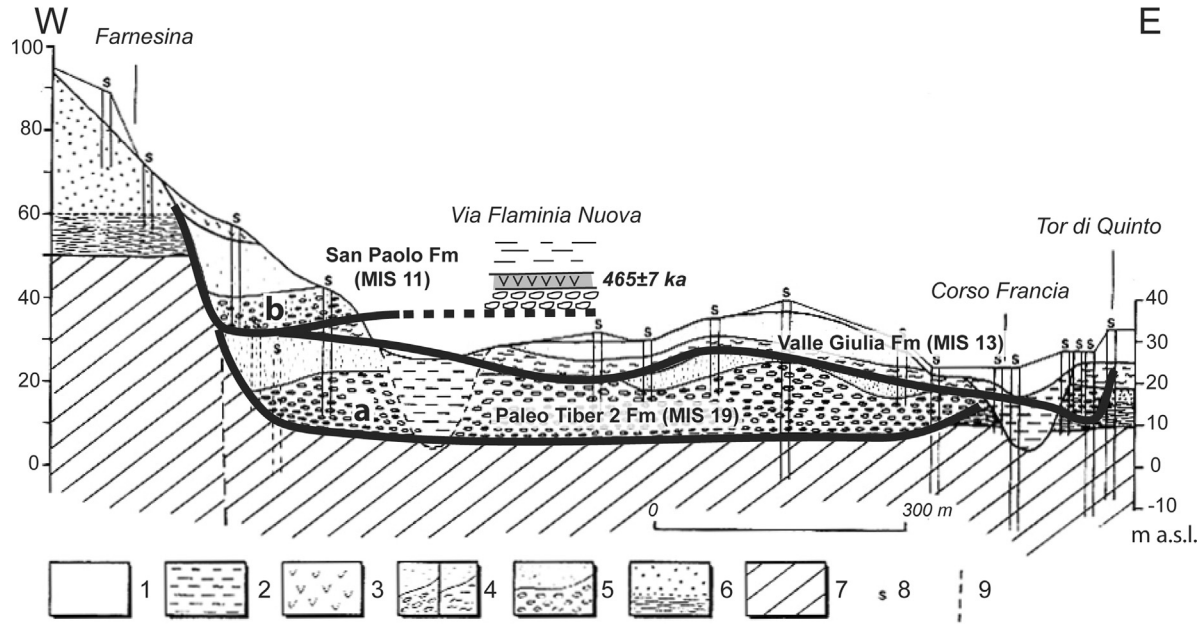

Fig. 7. Cross-section of the area north of Ponte Milvio, showing the occurrence of three aggradational cycles with gravel at the base (modified from Marra et al., 1995). Lateral correlation of the uppermost gravel layer with that cropping out in Via Flaminia Nuova, where a pyroclastic layer dated 465 ± 7 ka occurs (Karner and Renne, 1998), provides a link with MIS 11. The attribution of the second aggradational cycle to the Vale Giulia Formation and to MIS 13 is based on literature data on the sedimentary successions cropping out in Tor di Quinto and surrounding areas (Marra et al., 2014a). Correlation of the basal gravel layer to the Paleo-Tiber 2 succession (Marra and Florindo, 2014) is based on paleogeografic and stratigraphic considerations.

horizon of the San Paolo Formation. We correlate the tufaceous deposit from which the remains of rhinoceros were collected to this younger succession.

4.2.5. Tor di Quinto

The sedimentary deposits cropping out in Tor di Quinto, previously attributed along with similar deposits occurring in this northern sector of Rome to the "Parioliano" (e.g., Monte Antenne, Villa Glori, Val Melaina, Parioli; Ambrosetti and Bonadonna, 1967; Ambrosetti et al., 1972; Caloi and Palombo, 1988), have been assigned to the Valle Giulia Formation (Marra and Rosa, 1995) based on ages of intercalated volcanic deposits which allows correlation with MIS 14-13 (Karner and Marra, 1998). According to this interpretation, the large portion of the sedimentary deposits comprised between the two gravel layers "a" and "b" in Fig. 7, correlated respectively to MIS 20-21 and MIS 12-11, are attributed here to the Valle Giulia Formation, whose deposition spans 560–500 ka, considering deposition of the basal gravel to encompass also part of the regressive phase of MIS 14 (Karner and Marra, 1998).

4.2.6. Monte Verde

The Monte Verde area is an elevated sector rising to the west of the Tiber River alluvial plain, on the southern continuation of the N-S stretching Monte Mario-Gianicolo ridge. Here, several outcrops of Tufo Lionato, a lithified pyroclastic-flow deposit erupted 367 ± 4 ka by the Colli Albani volcanic district (Marra et al., 2009), form the flanks of the hills and was exploited since Roman times to produce dimension stone ("Tufo di Monteverde", Lugli, 1957). The collectors of the fossils are evidently referring to the tuff quarries as their provenance site.

Indeed, sandy and clayey, fluvial-lacustrine deposits of the Aurelia Formation, correlating to MIS 9 (Karner and Marra, 1998), caps the Tufo Lionato deposits in this area. Age of these sediments, and of the embedded fossils, is therefore comprised between that of the Tufo Lionato and that of the highstand of MIS 9 (0.37–0.33 Ma). Di Stefano et al. (1998) reported the occurrence of *Ursus deningeri* at Monte Verde, whose last occurrence in Italy is considered to correspond to MIS 11 (Gliozzi et al., 1997; Petronio et al., 2011). Nevertheless, according to the sediments age established here, the determination of the remains of *Ursus deningeri* should be revised, or the occurrence of this taxa in Italy prolonged to the MIS 10-9 (ca. 0.34 Ma).

4.2.7. Prati Fiscali; Monte Sacro, tufaceous conglomerates; Batteria Nomentana, levels covering the Tufo Lionato; Sedia del Diavolo, Vigna San Carlo, Vigne Torte

Fluvio-lacustrine sediments attributed to the Aurelia Formation (Marra and Rosa, 1995; Karner and Marra, 1998) extensively crop out on the hills forming the flanks of the Aniene River Valley in the northern area of Rome (Verri, 1915; Ventriglia, 1971). These outcrops comprise the fossiliferous localities of Monte Sacro and Prati Fiscali, to the north of the Aniene River, as well as Batteria Nomentana and Sedia del Diavolo, to the south (Fig. 1).

The upper portion of the sediments occurring at Sedia del Diavolo locality was attributed to the younger Vitinia Formation (correlating to MIS 7) based on the occurrence of an unconformity above where remains of *Dama dama tiberina* and *Equus hydruntinus* were collected (Palombo et al., 2004). In contrast, a geochronologic constraint provided by the distal pyroclastic-flow deposit of Tufo Giallo di Sacrofano, dated 287 ± 2 ka (Karner et al., 2001b), overlying the sedimentary successions in this sector, demonstrates that the upper deposit is a minor aggradational succession linked to the marine isotopic substage 8.5 (Via Mascagni subsequence; Marra et al., 2014a). Therefore, the age of the sediments of these cycles spans an interval from 0.367 (age of the Tufo Lionato pyroclastic-flow deposit; Marra et al., 2009) to 0.287 Ma. The same time span is attributed here to the sediments occurring at the localities of Vigna San Carlo and Vigne Torte, based on their correlation with the Aurelia Formation aggradational cycle, including the Via Mascagni subsequence, and on the recovered faunal assemblages.

4.2.8. Vitinia, upper levels, and Fosso di Malafede

Fossil remains from the type-section of the Vitinia Formation (Conato et al., 1980), as well as from the nearby Fosso di Malafede, have a precise radiometric constraint given by the age of 255 ± 5 ka (Karner and Renne, 1998) yielded by a pyroclastic layer intercalated in the sedimentary succession. This age allowed correlation of the sedimentary deposits with MIS 7 (Karner and Marra, 1998), whose duration encompasses the interval 0.25–0.19 Ma (Bassinot et al., 1994).

5. Discussion

Five Pleistocene species belonging to Rhinocerotidae are recorded in the fossiliferous deposits within the urban area of Rome (Table 1): *Stephanorhinus etruscus*, *S. hundsheimensis*, *S. hemitoechus*, *S. kirchbergensis*, and *Coelodonta antiquitatis*. The presences of an *Acerorhinus* species, testified by a reworked mandible (Pandolfi et al., 2013b), and *Stephanorhinus* aff. *hundsheimensis* are also reported in this area.

5.1. Stephanorhinus etruscus, S. hundsheimensis *and* S. *aff.* hundsheimensis

Stephanorhinus etruscus occurred in Italy during the latest Pliocene (Villafranca d'Asti; Guérin, 1980; Pandolfi, 2013) whereas its last occurrence is relatively controversial. Several small-sized remains from the latest Early Pleistocene of Europe were usually ascribed to *S. etruscus*, *S.* cf. *hundsheimensis* or *S. hundsheimensis* (Mazza et al., 1993; Lacombat, 2005; Made, 2010; Pandolfi and Petronio, 2011). According to Pandolfi and Petronio (2011), the latest Villafranchian Italian rhinoceroses can be ascribed to *S. etruscus*. The remains from Pietrafitta (latest Early Pleistocene, Farneta Faunal Unit *sensu* Gliozzi et al., 1997) were ascribed to *S.* cf. *S. hundsheimensis* by Mazza et al. (1993) and were related to *S. etruscus* by Made (2010), Pandolfi and Petronio (2011) and Pandolfi et al. (2015). Within the Roman area, *S. etruscus* is recorded only at Monte delle Piche. The revised chronology of that area enables us to provide an age of 0.86–0.82 Ma for the marine deposits at the bottom of the Monte delle Piche sequence (Fig. 2). This age represents the younger record of the Etruscan rhinoceros in Italy (Fig. 8). The last occurrence of *S. etruscus* can be therefore placed at the end of the Early Pleistocene and suggests a long persistence of the species in Italy, as for the Iberian Peninsula where it has been reported in the early Galerian localities of Huéscar (around 0.9 Ma) and Atapuerca TD4, TD6, and TD8 (Brunhes-Matuyama transition) (Cerdeño, 1993; Made, 1998, 1999, 2010; Fig. 8).

Stephanorhinus hundsheimensis is recorded in Europe during the latest Early and the Middle Pleistocene in several sites such as Vallonnet, Untermassfeld, Soleilhac, Mosbach, Isernia, La Pineta, and Mauer (Guérin, 1980; Fortelius et al., 1993; Kahlke, 2001; Schreiber, 2005; Lacombat, 2005; Fig. 8). According to Pandolfi and Petronio (2011) the first occurrence of the species in Italy was during the Early Galerian at Cava Redicicoli (north of Rome). The revision of the material collected from this locality and housed at MPUR confirms the occurrence of *S. hundsheimensis* at Cava Redicicoli. Nevertheless, the chronological attribution of the mammalian fauna discovered by Blanc (1955) in this locality has been a matter of debate (Di Stefano et al., 1998; Palombo et al.,

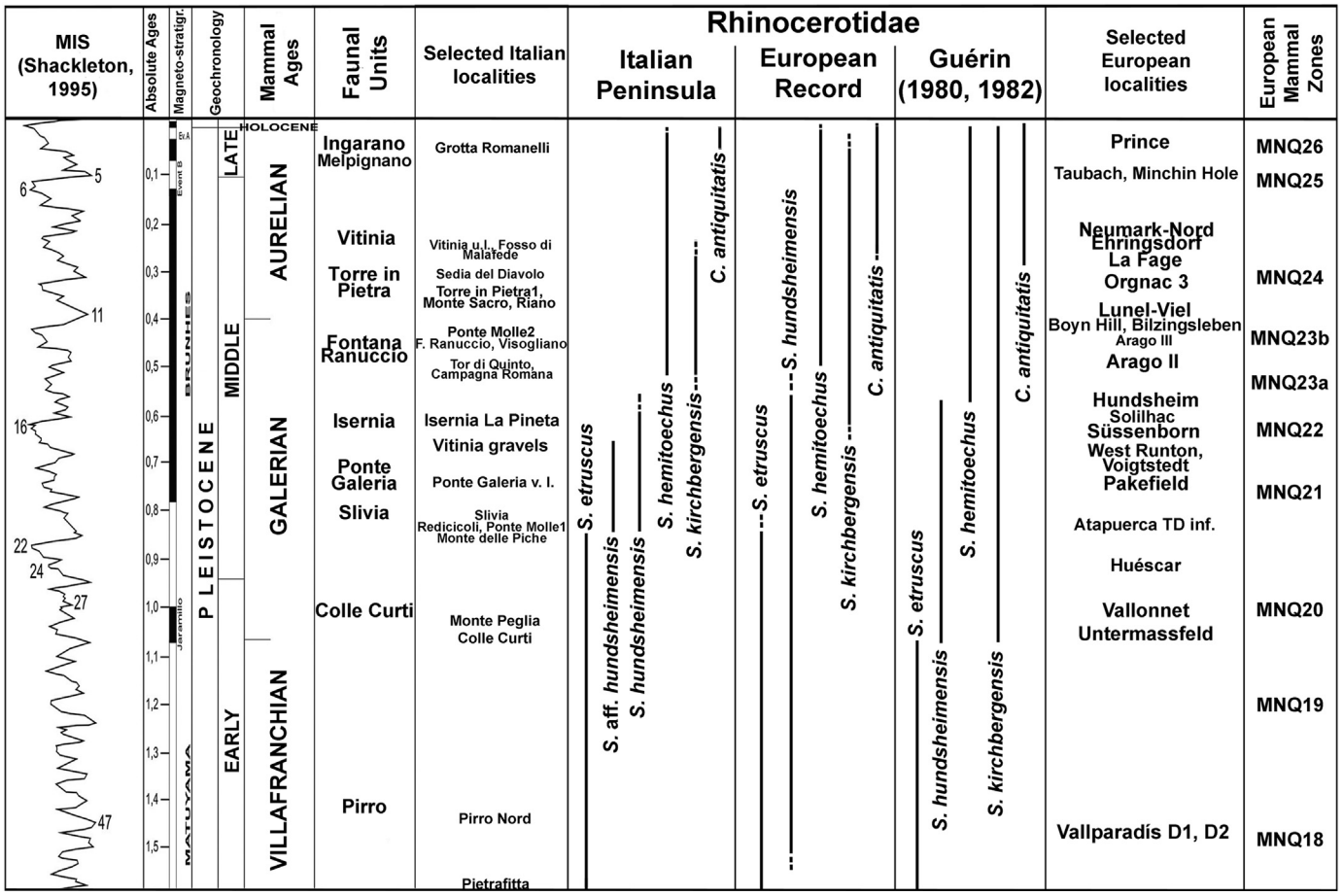

Fig. 8. New chronological scheme for the Pleistocene Italian rhinoceroses and comparison with the European record (see text for details) and Guérin's (1980, 1982) scheme (*S. hundsheimensis* = *D. etruscus brachycephalus* in Guérin, 1980, and *S. kirchbergensis* = *D. mercki* in Guérin, 1980).

2004; Milli and Palombo, 2005). Indeed, the reconstruction of the sub-surface stratigraphy in the larger area of Rome provided in Florindo et al. (2007) and Marra et al. (2014a) has shown that the alternating gravel and clay deposits underlying the early Alban Hills explosive products in the area north of Rome are those of the Paleo-Tiber 2 unit, which includes the PG1 and the Rome deposits, correlated to MIS 20-19 based on ages of two tephra layers dated at 802 and 788 ka (Florindo et al., 2007). Therefore, the faunal assemblage described there should be younger than the Colle Curti Local Fauna, dated at ca. 1.1 Ma. Palombo et al. (2002) and Milli and Palombo (2005) cited an unpublished manuscript of Blanc according to which the mammal assemblage came from a single fossiliferous level. This assemblage suggests a latest Early Pleistocene age for the deposits in which the remains were collected, and a correlation with the Colle Curti Faunal Unit has been proposed by Milli and Palombo (2005). Nevertheless, the occurrence of two distinct faunal assemblages in the Cava Redicicoli record, as suggested by Di Stefano et al. (1998), cannot be excluded also based on the detailed stratigraphic reconstruction of this area. According to Marra et al. (2014a), calcareous mud deposits correlated to MIS 17, as well as brown sandy silt deposits correlated to MIS 15, occur between the fluvial clay and gravel layers and the overlying volcanic deposits in the area north of Rome, and it is possible that the quarry where the vertebrate remains described by Blanc were discovered exposed the entire suite of these sedimentary sequences, which may have contained three faunal assemblages attributable to the Slivia, Ponte Galeria and Isernia Faunal Units (Marra et al., 2014a). Based on these considerations and the presence of *S. hundsheimensis* at the Slivia Local Fauna (Pandolfi and Petronio, 2011; Petronio et al., 2011; Pandolfi et al., 2013a), the earliest occurrence of the species can be placed around the Early-Middle Pleistocene transition (Fig. 8). Therefore, the earliest Italian record of *S. hundsheimensis* is younger than those from other European localities such as Vallonnet (France), Untermassfeld (Germany) and Vallparadís (Spain) (Kahlke, 2001; Moullé et al., 2006; Madurell-Malapeira et al., 2010; Fig. 8). Nevertheless, as noted by Pandolfi and Petronio (2011), the lack of remains clearly attributable to *S. hundsheimensis* before 1 Ma in Italy could be related to the scarcity of sites chronologically correlated with that time interval, even if delays of dispersal events due to the conformation of the Italian Peninsula cannot be ruled out (Pandolfi and Petronio, 2011).

Within the Roman area, *S. hundsheimensis* is also recorded from the gravels and sands of Ponte Molle referred to 0.81-0.79 Ma and Ponte Galeria referred to ca. 0.75 Ma (Marra et al., 2014a; Fig. 8). Based on the previous discussion about the chronology of Cava Redicicoli, the occurrence of *S. hundsheimensis* at Ponte Molle would be, together with that of Slivia, among the first sure presence of this species in the Italian Peninsula. From the gravels and sands of Ponte Molle and Vitinia, small-sized rhinoceros remains, slender than *S. hundsheimensis*, are recorded. These specimens are coeval in age with those referred to *S. hundsheimensis* but can be related to a different taxon. Unfortunately, the scant material and the absence of cranial elements do not allow an exhaustive comparison and therefore an accurate taxonomic attribution. The Toula species disappeared

from the Italian Peninsula during the MIS 15-16 and it was replaced by *S. hemitoechus* (Pandolfi et al., 2013a).

5.2. Stephanorhinus hemitoechus *and* S. kirchbergensis

The earliest occurrence of *S. hemitoechus* in Italy has been recently reported by Pandolfi et al. (2013a) from the Campagna Romana, approximately at 0.5 Ma; the species was relatively common in several late Middle and Late Pleistocene Italian localities (Guérin, 1980; Pandolfi et al., 2013a; Pandolfi and Tagliacozzo, 2015; Fig. 8). In the urban area of Rome, *S. hemitoechus* is recorded at Ponte Molle tufaceous conglomerates, Sedia del Diavolo, Monte Sacro, Vigna San Carlo, Vitinia upper levels, and Fosso di Malafede, thus suggesting a continuous presence of the species in that area. The chronological constrains on the Ponte Molle tufaceous conglomerate deposits support an age older than 0.4 Ma for the occurrence of the species in Italy, in agreement with Pandolfi et al. (2013a).

In Spain and Portugal, *S. hemitoechus* is the only species of the genus present during the late Middle and Late Pleistocene (Cerdeño, 1990; Cardoso, 1993; Marks et al., 2002; Lacombat, 2005; Made, 2010). Its appearance in the Iberian Peninsula is referable to approximately 0.4 Ma (Cerdeño, 1990; Sesé and Soto, 2005; Made, 2010). In central and northern Europe, *S. hemitoechus* is sometimes reported in association with *S. kirchbergensis* and/or *C. antiquitatis* (sites of La Fage and Neumark-Nord; Guérin, 1973, 1980; Schreve, 1996; Made, 2010). *S. hemitoechus* was first recorded in Great Britain during MIS 11 (ca. 0.4 Ma) together with *S. kirchbergensis* (Boyn Hill and Orsett Heath sites; Schreve, 1996, Bridgland et al., 2004) and both species are coeval at the site of Bilzingsleben (Germany) (Made, 2000, 2010; Bridgland et al., 2004) and several other localities dated to the late Middle Pleistocene and the earliest Late Pleistocene (La Fage, Neumark-Nord, Burgtonna, Ehringsdorf, Grotte du Prince; Guérin, 1973; Kahlke, 1977; 1980; Lacombat, 2005; Made, 2010; Fig. 8). *S. kirchbergensis* and *S. hemitoechus* co-occur in Italy only in the fossiliferous deposits of the Roman area at Ponte Molle tufaceous conglomerates and maybe at Sedia del Diavolo.

According to Billia and Petronio (2009), the first occurrence of *S. kirchbergensis* in Italy can be referred to the Isernia Faunal Unit, in the site of Ponte Molle. However, most specimens from Ponte Molle described by Billia and Petronio (2009) lack stratigraphic information on their labels. Pandolfi et al. (2013a) and Pandolfi (2013) recently suggested that the earliest occurrence of *S. kirchbergensis* in Italy was at Visogliano, referable to MIS 12. The chronological constraint for the tufaceous conglomerates at Ponte Molle, which span from 0.46 Ma to 0.43 Ma, supports this hypothesis. However, the species is also recorded in the sedimentary deposits at Tor di Quinto, which, according to our intepretetion, are slightly older than the tufaceous conglomerate levels of Ponte Molle. Therefore, the Tor di Quinto record is currently the earliest evidence of *S. kirchbergensis* in Italy.

5.3. Coelodonta antiquitatis

According to Kahlke and Lacombat (2008), the first occurrence of the genus *Coelodonta* in Europe is in deposits of a glacial meltwater delta of MIS 12 (about 460 ka in age) in the site of Bad Frankenhausen. However, this record has been questioned by Guérin (2010). The woolly rhino is a common element in all European cold stages until the Late Pleistocene, and even under moderate temperatures when it is dry enough (Guérin, 1980; Kahlke and Lacombat, 2008). During the last glacial maximum, the woolly rhino was present from Iberian Peninsula to Siberia and from Scotland to Greece (Melentis, 1966; Borsuk-Bialynicka, 1973; Guérin, 1980; Kahlke, 1999; Orlova et al., 2004). In Italy, it is recorded only in a few localities, often lacking stratigraphic or chronological data. The species is represented by tooth remains at Opcina, Fadalto nel Veneto, Polesine (Leonardi, 1947, 1947–48), and Riparo Fumane (Cremaschi et al., 2005); by a fragmentary skull at Monte Circeo (Palmarelli and Palombo, 1981); and by several remains at Settepolesini di Bondeno (Gallini and Sala, 2001), Ingarano (Petronio and Sardella, 1998), Cardamone (Vaufrey, 1927), and Grotta Romanelli (Pandolfi and Tagliacozzo, 2013). The earliest record of woolly rhino in Italy was chronologically comprised between 80 and 69 ka (Grotta Romanelli; Pandolfi and Tagliacozzo, 2013; Fig. 8). The species is scarcely documented in the Tyrrhenian side of the Peninsula, where it is only testified by the record of Monte Circeo.

The present paper shows, for the first time, the presence of *C. antiquitatis* in the Roman area. This occurrence suggests the presence of fossiliferous deposits chronologically related to a glacial phase of the Pleistocene. The presence of fossil remains referable to cold stages, most probably MIS 4-3 or maybe MIS 6, should be regarded as an uncommon occurrence in the area of Rome, where the sedimentary record is represented by discontinuous aggradational successions mainly deposited during periods of sea-level rise. Indeed, the continued retreat of the coastline during periods of sea-level lowering causes incision of the fluvial valleys, preventing sediment accumulation. However, as already discussed in Marra et al. (2014a), deposition of the basal gravel layers of these successions may encompass a portion of the late glacial period, or early aggradations may occur in response to minor oscillations during the sub-stages of the Oxygen isotopes curve (Marra and Florindo, 2014). Nevertheless, the deposits of MIS 6 and MIS 4-3, whenever preserved, should be presently buried below those of the following, larger eustatic cycle of MIS 2-1, which caused deep erosion and the successive filling of the hydrographic network of the Tiber River and its tributaries by several ten-meter thick packages of sediments (Marra et al., 2013).

The reference to a provenance from the Tiber River "terraces" may explain the nature and the genesis of the deposits in which these fossils remain occurred. Marine terraces of MIS 7 and MIS 5 along the coast of Rome at ca. 45 and ca. 25 m a.s.l., respectively (Hearty and Dai-Pra, 1986; Sorgi, 1994), reflect the occurrence of a regional uplift of ca. 50 m during the last 250 k.y. (Karner et al., 2001a). The related fluvial deposits of these cycles are scarcely present or lacking in the area of Rome due to their erosion, also as a consequence of the tectonic uplift (Marra et al., 2014a). The only known occurrence of deposits correlated to MIS 5 is that of a "Tyrrhenian terrace" along the Aniene River valley, in which a skull of *Homo neanderthalensis* was recovered (Blanc, 1939). Similarly, terraces of MIS 6-5 and 4-3 may be preserved as relic sedimentary bodies along the flanks of the major Tiber River valley.

6. Conclusions

Several rhinoceros remains were collected in the urban area of Rome, in particular between the end of the 19th century and the beginning of the 20th century. These remains were mainly found in the fluvial deposits of the Tiber and Aniene Rivers and were mentioned in several contributions (e.g., Caloi et al., 1998; Di Stefano et al., 1998; Palombo et al., 2002; Milli and Palombo, 2005; Kotsakis and Barisone, 2008), but without a careful taxonomic revision. In addition, by establishing correlation of the sedimentary sections hosting the fossil remains with the geochronologically-constrained, astronomically-forced aggradational successions of the Paleo-Tiber River, the fossil remains are framed within a detailed chronostratigraphic scheme without equivalent in the previous literature.

The paleontological analysis of the rhinoceros remains allows the identification of five species: *Stephanorhinus etruscus*, *S. hundsheimensis*, *S. hemitoechus*, *S. kirchbergensis*, and *Coelodonta antiquitatis*. The records of an undeterminated *Acerorhinus* species and a smaller undeterminated *Stephanorhinus* species are also reported from the urban area of Rome.

The specimen ascribed to *S. etruscus* was collected from the marine deposit at Monte delle Piche, which age spans between 0.86 and 0.82 Ma. The Monte delle Piche record is the younger evidence of the presence of *S. etruscus* in Italy (Fig. 8). This species was usually reported from several Villafranchian fossiliferous localities of Europe, but only in Spain it was recorded until the Matuyama/Brunhes transition (Cerdeño, 1993; Made, 1998, 1999, 2010; Fig. 8). The long persistence of *S. etruscus* in both Italian and Iberian Peninsula may be related to the role of "refugia" played by both areas. However, the persistence of stable and favourable climatic and ecological conditions for the species during the beginning of a major transformation of the climatic and vegetational cycles ("Mid-Pleistocene Revolution"), coincident with the passage to an astronomical phase characterised by 100-k.y. glacial cycles (Leroy, 2007; Alonso-García et al., 2011; Joannin et al., 2011; Leroy et al., 2011; McClymont et al., 2013), cannot be ruled out. During this time, *S. hundsheimensis* occurred in the Italian Peninsula as testified by the records of Slivia and Ponte Molle gravels and sands (Pandolfi and Petronio, 2011; Pandolfi, 2013; Fig. 8). The dispersal event of *S. hundsheimensis* into central Europe and later in Italy may be related to the climatic deterioration of the latest Early Pleistocene and to a greater capacity of the species to adapt to the climatic conditions and diet (with highly flexible feeding; Kahlke and Kaiser, 2011) than *S. etruscus*. In Italy, *S. hundsheimensis* disappeared before ca. 0.5 Ma, when *S. hemitoechus* appeared for the first time (Pandolfi et al., 2013a; Fig. 8).

The first occurrence of *S. kirchbergensis* in Italy is here reported in Middle Pleistocene deposits at Tor di Quinto, but the species occurred slightly earlier in Europe, at Solilhac (MIS 15; Guérin, 1980; Lacombat, 2005; Fig. 8). The dispersal of this species could be related to the expansion of forest environments; this hypothesis is supported by the brachydont teeth of this species and by the remains of flora and fauna that have been discovered together with it (Guérin, 1980). The occurrence of this species in the diatomaceous deposit at Riano (north of Rome; MIS 10?; Gliozzi et al., 1997; Pandolfi, 2011b; Petronio et al., 2011), together with an abundant fossil flora characterising a dense forest (Follieri, 1958a, 1958b, 1962; Follieri and Magri, 2001), is in agreement with previous studies which suggest the forest affinities of *S. kirchbergensis* (Loose, 1975; Fortelius et al., 1993; Tong and Wu, 2010). This may explain the absence of this species in Southern Italy, in the Iberian Peninsula and in Northern Africa, unlike *S. hemitoechus* (Guérin, 1980; Cerdeño, 1990; Billia and Petronio, 2009; Pandolfi et al., 2013a).

C. antiquitatis is rarely recorded in Italy, and it is mainly reported in Apulia or in Northern Italy. Despite the lack of detailed information on the locality, findings of this species from the Tiber River deposits add a new contribution on its knowledge and provide the evidence that the woolly rhinoceros was probably more widespread in the Italian Peninsula than previously reported.

A few specimens collected from the fossiliferous deposits within the urban area of Rome suggest the presence of a small species during the early Middle Pleistocene, which is slender than the coeval *S. hundsheimensis*. Nevertheless, new material is needed for an exhaustive analysis and any taxonomic consideration about these specimens is prevented at this time.

Acknowledgment

We thank two anonymous reviewers and Dr. O. Sanisidro for insightful suggestions and comments on the manuscript. We also thank the editors Pr. P.-O. Antoine and Dr. G. Escarguel. L.P. thanks M. Gasparik (HNHM), E. Cioppi (IGF), E. Bodor (MFGI), O. Hampe (MfN), C. Sarti (MGGC), M. Fornasiero (MGPP), P. Pérez Dios (MNCN), A. Tagliacozzo (MNPELP), C. De Angelis (MPLBP), R. Manni and C. Petronio (MPUR; the specimens were studied between 2008 and 2010), F. Farsi (MSNAF), P. Agnelli (MSNF), R. Francescangeli and V. Montenegro (MSTB), P. Brewer (NHML), U. Göhlich (NHMW), and L. Costeur (NMB) for their help and assistance during his visits to the rhinoceros fossil collections. L.P. also thanks L. Maiorino and G. Sansalone for sending pictures of specimens housed in several Institutions. L.P. thanks the European Commission's Research Infrastructure Action, EU-SYNTHESYS project AT-TAF-2550, DE-TAF-3049, GB-TAF-2825, HU-TAF-3593, and ES-TAF-2997. Part of this research received support from the SYNTHESYS Project (http://www.synthesys.info/), which is financed by European Community Research Infrastructure Action under the FP7 "Capacities" Program.

References

Alonso-García, M., Sierro, F.J., Kucera, M., Flores, J.A., Cacho, I., Andersen, N., 2011. Ocean circulation, ice sheet growth and inter-hemispheric coupling of millennial climate variability during the mid-Pleistocene (ca 800–400 ka). Quaternary Science Reviews 30, 3234–3247.

Ambrosetti, P., 1967. Cromerian fauna of the Rome Area. Quaternaria 9, 267–283.

Ambrosetti, P., Bonadonna, F.P., 1967. Revisione dei dati sul Plio-Pleistocene di Roma. Atti della Società Gioenia di Scienze Nataturali di Catania 18, 33–72.

Ambrosetti, P., Azzaroli, A., Bonadonna, F.P., Follieri, M., 1972. A scheme of Pleistocene Chronology for the Tyrrhenian side of Central Italy. Bollettino della Società Geologica Italiana 91, 169–184.

Antoine, P.-O., 2002. Phylogenie et évolution des Elasmotheriina (Mammalia, Rhinocerotidae). Memoires du Muséum National d'Histoire Naturelle Paris 188, 1–353.

Bassinot, F.C., Labeyrie, L.D., Vincent, E., Quidelleur, X., Shackleton, N.J., Lancelot, Y., 1994. The astronomical theory of climate and the age of the Brunhes-Matuyama magnetic reversal. Earth and Planetary Science Letters 126, 91–108.

Billia, E.M.E., Petronio, C., 2009. Selected records of *Stephanorhinus kirchbergensis* (Jäger, 1839) (Mammalia, Rhinocerotidae) in Italy. Bollettino della Società Paleontologica Italiana 48, 1–12.

Blanc, A.C., 1939. Il giacimento musteriano di Saccopastore nel quadro del Pleistocene Laziale. Rivista di Antropologia 32, 223–234.

Blanc, A.C., 1955. Ricerche sul Quaternario Laziale, III. Avifauna artica, crioturbazioni e testimonianze di soliflussi nel Pleistocene medio-superiore di Roma e di Torre in Pietra. Il periodo glaciale Nomentano, nel quadro della serie di glaciazioni riconosciute nel Lazio. Quaternaria 2, 187–200.

Blumenbach, J.F., 1799. Handbuch der Naturgeschichte. Sechste Ausgabe. In: Göttingen, Johann Christian Dieterich. 6th Ed (pp. i–xvi, 1–703).

Bonadonna, F.P., 1968. Studi sul Pleistocene del Lazio. V. La Biostratigrafia di Monte Mario e la "Fauna Malacologica Mariana" di Cerulli-Irelli. Memorie della Società Geologica Italiana 7, 261–321.

Borsuk-Bialynicka, M., 1973. Studies on the Pleistocene rhinoceros *Coelodonta antiquitatis* (Blumenbach). Palaeontologia Polonica 29, 97.

Bridgland, D.R., Schreve, D.C., Keen, D.H., Meyrick, R., Westaway, R., 2004. Biostratigraphical correlation between the late Quaternary sequence of the Thames and key fluvial localities in central Germany. Proceedings of the Geologists' Association 115, 125–140.

Caloi, L., Palombo, M.R., 1988. Le mammalofaune plio-pleistoceniche dell'area laziale: problemi biostratigrafici ed implicazioni paleoclimatiche. Memorie della Società Geologica Italiana 35, 99–126.

Caloi, L., Palombo, M.R., Petronio, C., 1979. Cenni preliminari sulla fauna di Cava Redicicoli (Roma). Bollettino del Servizio Geologico Italiano 100, 189–198.

Caloi, L., Palombo, M.R., Petronio, C., 1980. La fauna quaternaria di Sedia del Diavolo (Roma). Quaternaria 22, 177–209.

Caloi, L., Palombo, M.R., Zarlenga, F., 1998. Late Middle Pleistocene mammal faunas of Latium-Stratigraphy and environment. Quaternary International 47/48, 77–86.

Caloi, L., Cuggiani, M.C., Palmarelli, A., Palombo, M.R., 1981. La fauna a Vertebrati del Pleistocene medio e superiore di Vitinia (Roma). Bollettino del Servizio Geologico Italiano 102, 41–76.

Cardoso, J.L., 1993. Contribuíçao para o conhecímento dos grandes mamiferos do Plístocéníco superior de Portugal. Cámara Municipal de Oeiras.

Cerdeño, E., 1990. *Stephanorhinus hemitoechus* (Falc.) (Rhinocerotidae, Mammalia) del Pleistoceno Medio y Superior de España. Estudios Geologicos 46, 465–479.

Cerdeño, E., 1993. Remarks on the Spanish Plio-Pleistocene *Stephanorhinus etruscus* (Rhinocerotidae). Comptes Rendus de l'Académie des Sciences de Paris 317, 1363–1367.

Conato, V., Esu, D., Malatesta, A., Zarlenga, F., 1980. New data on Pleistocene of Rome. Quaternaria 22, 131–176.

Cosentino, D., Cipollari, P., Di Bella, L., Esposito, A., Faranda, C., Giordano, G., Mattei, M., Mazzini, I., Porreca, M., Funiciello, R., 2009. Tectonics, sea-level changes and palaeoenvironments in the early Pleistocene of Rome (Italy). Quaternary Research 72, 143–155.

Cremaschi, M., Ferraro, F., Peresani, M., Tagliacozzo, A., 2005. Il sito: nuovi contributi sulla stratigrafia, la cronologia, le faune a macromammiferi e le industrie del paleolitico antico. In: Broglio, A., Dalmeri, G. (Eds.), Pitture paleolitiche nelle Prealpi Venete: Grotta di Fumane e Riparo Dalmeri, Atti del Simposio, Memorie Museo Civico di Storia Naturale di Verona, 2° serie (Sezione Scienze dell'Uomo 9). Preistoria Alpina, numero speciale, pp. 12–22.

De Christol, J., 1834. Recherches sur les caractères des grandes espèces de Rhinocéros fossiles. Annales des Sciences naturelles, Paris, s. 2 (4), 44–112.

Di Stefano, G., Petronio, C., Sardella, R., 1998. Biochronology of the Pleistocene mammal faunas from Rome urban area. Il Quaternario 11, 191–199.

Falconer, H., 1859. In Gaudin C.T. (1859), Modifications apportées par Mr. Falconer à la faune du Val d'Arno. Bulletin de la Société Vaudoise des Sciences Naturelles 6, 130–131.

Falconer, H., 1868. On the European Pliocene and Post-Pliocene species of the genus Rhinoceros. In: Palaeontological Memoirs and Notes of the late Hugh Falconer, compiled and edited by Charles Murchison, London, Robert Hardwicke (2) Mastodon, Elephant, Rhinoceros, Ossiferous Caves, Primeval Man and His Cotemporaries. 309–403.

Florindo, F., Karner, D.B., Marra, F., Renne, P.R., Roberts, A.P., Weaver, R., 2007. Radioisotopic age constraints for Glacial Terminations IX and VII from aggradational sections of the Tiber River delta in Rome, Italy. Earth and Planetary Science Letters 256, 61–80.

Follieri, M., 1958a. Notizie preliminari su una flora fossile a *Pterocarya* rinvenuta nelle diatomiti di Riano. Annali di Botanica 26, 1–3.

Follieri, M., 1958b. La foresta colchica fossile di Riano Romano. I. – studio dei fossili vegetali macroscopici. Annali di Botanica 26, 129–142.

Follieri, M., 1962. La foresta colchica fossile di Riano Romano. II – analisi polliniche. Annali di Botanica 27, 245–280.

Follieri, M., Magri, D., 2001. Middle and Upper Pleistocene natural environment in the Roman area: climate, vegetation and landscape. In: Cavarretta, G., Gioia, P., Mussi, M., Palombo, M.R. (Eds.), La Terra degli Elefanti. Atti 1° Congresso Internazionale, Università Sudi Roma La Sapienza, Roma, pp. 43–47.

Fortelius, M., 1981. The rhinoceros from Sedia Diavolo (Rome) is *Dicerorhinus hemitoechus*. Quaternaria 23, 143–144.

Fortelius, M., Mazza, P., Sala, B., 1993. *Stephanorhinus* (Mammalia, Rhinocerotidae) of the western European Pleistocene, with a special revision of *Stephanorhinus etruscus* (Falconer, 1868). Palaeontographia Italica 80, 63–155.

Gallini, V., Sala, B., 2001. Settepolesini di Bondeno (Ferrara – Eastern Po Valley): the first example of mammoth steppe in Italy. In: Cavarretta, G., Gioia, P., Mussi, M., Palombo, M.R. (Eds.), Proceedings of the 1st International Congress "The World of Elephants", Rome October 16–20, 2001. CNR (Consiglio Nazionale delle Ricerche) Publishing House, Roma, pp. 247–254.

Gibbard, P.L., Head, M.J., Walker, M.J.C., The subcommission on Quaternary Stratigraphy, 2010. Formal ratification of the Quaternary System/Period and the Pleistocene Series/Epoch with a base at 2.58 Ma. Journal of Quaternary Science 25, 96–102.

Gliozzi, E., Abbazzi, L., Ambrosetti, P.G., Argenti, P., Azzaroli, A., Caloi, L., Capasso Barbato, L., Di Stefano, G., Ficcarelli, G., Kotsakis, T., Masini, F., Mazza, P., Mezzabotta, C., Palombo, M.R., Petronio, C., Rook, L., Sala, B., Sardella, R., Zanalda, E., Torre, D., 1997. Biochronology of selected mammals, molluscs and ostracods from the Middle Pliocene to the Late Pleistocene in Italy. The state of the art. Rivista Italiana di Paleontologia e Stratigrafia 103, 369–388.

Goddard, J., 1970. Age criteria and vital statistics of a black rhinoceros population. East African Wildlife Journal 8, 105–121.

Guérin, C., 1972. Une nouvelle espèce de Rhinocéros (Mammalia, Perissodactyla) à Vialette (Haute-Loire, France) et dans d'autres gisements du Villafranchien Inférieur Européen: *Dicerorhinus jeanvireti* n. sp. Documents des Laboratoires de Géologie de la Faculté des Sciences de Lyon 49, 53–161.

Guérin, C., 1973. Les trois espèces de Rhinocéros (Mammalia, Perissodactyla) du gisement Pléistocène Moyen des Abimes de La Fage a Noailles (Corrèze). Nouvelles Archives Museum Histoire Naturelle de Lyon 11, 55–84.

Guérin, C., 1980. Les rhinocéros (Mammalia, Perissodactyla) du Miocène terminal au Pléistocène supérieur en Europe occidentale. Comparaison avec les espèces actuelles. Documents du Laboratoire de Géologie de Lyon 79, 1–1185.

Guérin, C., 2010. *Coelodonta antiquitatis praecursor* (Rhinocerotidae) du Pléistocène moyen final de l'aven de Romain-la-Roche (Doubs, France). Revue de Paléobiologie, Genève 29, 697–746.

Hearty, P.J., Dai-Pra, G., 1986. Aminostratigraphy of Quaternary marine deposits in the Lazio region of central Italy. In: Ozer, A., Vita-Finzi, C. (Eds.), Dating Mediterranean shorelines. Supplementband 62. Zeitschrift fuer Geomorphologie, pp. 131–140.

Hillman-Smith, A.K.K., Owen-Smith, N., Anderson, J.L., Hall-Martin, A.J., Selaladi, J.P., 1986. Age estimation of the White rhinoceros (*Ceratotherium simum*). Journal of Zoology London, Series A 210, 355–379.

Jäger, G.F., 1835–1839. Über die fossilen Säugetiere welche in Württemberg in verschiedenen Formationen aufgefunden worden sind, nebst geognotischen Bemerkungen über diese Formtionen. C. Erhard Verlag, Stuttgart.

Joannin, S., Bassinot, F., Nebout, N.C., Peyron, O., Beaudouin, C., 2011. Vegetation response to obliquity and precession forcing during the Mid-Pleistocene Transition in Western Mediterranean region (ODP site 976). Quaternary Science Reviews 30, 280–297.

Kahlke, H.-D., 1977. Die Rhinocerotidenreste aus den Travertinen von Taubach. Quartärpaläontologie 2, 305–359.

Kahlke, R.-D., 1999. The History of the Origin. In: Evolution and Dispersal of the Late Pleistocene Mammuthus-Coelodonta Faunal Complex in Eurasia (Large Mammals). Fenske Companies, Rapid City.

Kahlke, R.-D., 2001. Die Rhinocerotiden-Reste aus dem Unterpleistozän von Untermaßfeld. In: Kahlke, R.-D. (Ed.), Das Pleistozän von Untermaßfeld bei Meiningen (Thüringen). Teil 2, Habelt, Mainz 40, pp. 501–555.

Kahlke, R.-D., Lacombat, F., 2008. The earliest immigration of woolly rhinoceros (*Coelodonta lologoijensis*, Rhinocerotidae, Mammalia) into Europe and its adaptative evolution in Palaearctic cold stage mammal faunas. Quaternary Science Reviews 27, 1951–1961.

Kahlke, R.-D., Kaiser, T.K., 2011. Generalism as a subsistence strategy – Advantages and limitations of the highly flexible feeding traits of Pleistocene *Stephanorhinus hundsheimensis* (Rhinocerotidae, Mammalia). Quaternary Science Reviews 30, 2250–2261.

Karner, D.B., Marra, F., 1998. Correlation of fluviodeltaic aggradational sections with glacial climate history: a revision of the classical Pleistocene stratigraphy of Rome. Geological Society of American Bulletin 110, 748–758.

Karner, D.B., Renne, P.R., 1998. $^{40}Ar/^{39}Ar$ geochronology of Roman volcanic province tephra in the Tiber River valley: age calibration of Middle Pleistocene sea-level changes. Geological Society of American Bulletin 110, 740–747.

Karner, D.B., Marra, F., Florindo, F., Boschi, E., 2001a. Pulsed uplift estimated from terrace elevations in the coast of Rome: evidence for a new phase of volcanic activity? Earth and Planetary Science Letters 188, 135–148.

Karner, D.B., Marra, F., Renne, P.R., 2001b. The history of the Monti Sabatini and Alban Hills volcanoes: groundwork for assessing volcanic-tectonic hazards for Rome. Journal of Volcanology and Geothermal Research 107, 185–215.

Kaup, J.-J., 1832. Über *Rhinoceros incisivus* Cuvier und eine neue Art, *Rhinoceros schleiermacheri*. Isis 8, 898–904.

Koenigswald, W. von, Holly Smith, B., Keller, Th., 2007. Supernumerary teeth in a subadult rhino mandible (*Stephanorhinus hundsheimensis*) from the Middle Pleistocene of Mosbach in Wiesbaden (Germany). Palaeontologische Zeitschrift 81, 416–428.

Kotsakis, T., Barisone, G., 2008. I vertebrati fossili continentali del Plio-Pleistocene dell'area romana. In: Funiciello, R., Praturlon, A., Giordano, G. (Eds.), La Geologia di Roma, Memorie Descrittive della Carta Geologica d'Italia, 80, pp. 115–143.

Kretzoi, M., 1942. Bemerkungen zum System der nachmiozänen Nashorn-Gattungen. Földtani Közlöny 72, 309–318.

Kuiper, K.F., Deino, A., Hilgen, F.J., Krijgsman, W., Renne, P.R., Wijbrans, J.R., 2008. Synchronizing rock clocks of Earth history. Science 320, 500–505.

Lacombat, F., 2005. Les rhinocéros fossiles des sites préhistoriques de l'Europe méditerranéenne et du Massif central. Paléontologie et implications biochronologiques. BAR International Series 1419, 1–175.

Lacombat, F., 2006. Morphological and biometrical differentiation of the teeth from Pleistocene species of *Stephanorhinus* (Mammalia, Perissodactyla, Rhinocerotidae) in Mediterranean Europe and Massif Central, France. Palaeontographica Abteilung A: Paläozoologie–Stratigraphie 274, 71–111.

Leonardi, P., 1947. Resti fossili di rinoceronti del Museo di Storia Naturale di Trieste. Atti del Museo Civico di Storia Naturale di Trieste 16, 145–164.

Leonardi, P., 1947–1948. Resti fossili inediti di rinoceronti conservati nelle collezioni dell'Istituto Geologico dell'Università di Padova. Memorie dell'Istituto di Geologia dell'Università di Padova 15, 1–30.

Leroy, S.A.G., 2007. Progress in palynology of the Gelasian-Calabrian Stages in Europe: ten messages. Revue de Micropaléontologie 50, 293–308.

Leroy, S.A.G., Arpe, K., Mikolajewicz, U., 2011. Vegetation context and climatic limits of the Early Pleistocene hominin dispersal in Europe. Quaternary Science Review 30, 1448–1463.

Lisiecki, L.E., Raymo, M.E., 2005. A Pliocene-Pleistocene stack of 57 globally distributed benthic (18O records. Paleoceanography 20,, http://dx.doi.org/10.1029/2004PA001071 PA 1003.

Loose, H., 1975. Pleistocene Rhinocerotidae of W. Europe with reference to the recent two-horned species of Africa and S.E. Asia. Scripta Geologica 33, 1–59.

Lugli, G., 1957. La tecnica edilizia romana con particolare riguardo a Roma e Lazio. Bardi, Rome743.

Made, J. van der, 1998. Ungulates from Gran Dolina (Atapuerca, Burgos, Spain). Quaternaire 9, 267–281.

Made, J. van der, 1999. Ungulates from Atapuerca-TD6. Journal of Human Evolution 37, 389–413.

Made, J. van der, 2000. A preliminary note on the rhinos from Bilzingsleben. Praehistoria Thuringica 4, 41–64.

Made, J. van der, 2010. The rhinos from the Middle Pleistocene of Neumark-Nord (Saxony-Anhalt). In: Neumark-Nord: Ein interglaziales Ökosystem des mittelpaläolithischen Menschen. Veröffentlichungen des Landesmuseums für Vorgeschichte 62. 433–527.

Madurell-Malapeira, J., Minwer-Barakat, R., Alba, D.M., Garcés, M., Gómez, M., Aurell-Garrido, J., Ros-Montoya, S., Moyà-Solà, S., Berástegui, X., 2010. The Vallparadís section (Terrassa, Iberian Peninsula) and the latest Villafranchian faunas of Europe. Quaternary Science Reviews 29, 3972–3982.

Marks, A.E., Brugal, J.P., Chabai, V.P., Monigal, K., Goldberg, P., Hockett, B., Peman, E., Elorza, M., Malloll, C., 2002. Le gisement Pléistocène moyen de Galeria Pesada, (Estrémadure, Portugal): premiers résultats. Paléo 14, 77–100.

Marra, F., Rosa, C., 1995. Stratigrafia e assetto geologico dell'area romana. Memorie Descrittive della Carta Geologica d'Italia 50, 49–118.
Marra, F., Carboni, M.G., Di Bella, L., Faccenna, C., Funiciello, R., Rosa, C., 1995. Il substrato plio-pleistocenico nell'Area Romana. Bollettino della Società Geologica Italiana 114, 195–214.
Marra, F., Florindo, F., 2014. The subsurface geology of Rome: sedimentary processes, sea-level changes and astronomical forcing. Earth-Science Reviews 136, 1–20.
Marra, F., Florindo, F., Karner, D.B., 1998. Paleomagnetism and geochronology of early Middle Pleistocene depositional sequences near Rome: comparison with the deep sea d^{18}O climate record. Earth and Planetary Science Letters 159, 147–164.
Marra, F., Florindo, F., Boschi, E., 2008. The history of glacial terminations from the Tiber River (Rome): insights to glacial forcing mechanisms. Paleoceanography 23, PA2205, http://dx.doi.org/10.1029/2007PA001543.
Marra, F., Bozzano, F., Cinti, F.R., 2013. Chronostratigraphic and lithologic features of the Tiber River sediments (Rome, Italy): implications on the Post-glacial sea-level rise and Holocene climate. Global and Planetary Change 107, 157–176.
Marra, F., Karner, D.B., Freda, C., Gaeta, M., Renne, P.R., 2009. Large mafic eruptions at the Alban Hills Volcanic District (Central Italy): chronostratigraphy, petrography and eruptive behavior. Journal of Volcanology and Geothermal Research 179, 217–232.
Marra, F., Pandolfi, L., Petronio, C., Di Stefano, G., Gaeta, M., Salari, L., 2014a. Reassessing the sedimentary deposits and vertebrate assemblages from Ponte Galeria area (Rome, central Italy): an archive for the Middle Pleistocene faunas of Europe. Earth-Science Reviews 139, 104–122.
Marra, F., Sottili, G., Gaeta, M., Giaccio, B., Jicha, B., Masotta, M., Palladino, D.M., Deocampo, D., 2014b. Major explosive activity in the Sabatini Volcanic District (central Italy) over the 800–390 ka interval: geochronological–geochemical overview and tephrostratigraphic implications. Quaternary Science Reviews 94, 74–101.
Mazza, P., Sala, B., Fortelius, M., 1993. A small latest Villafranchian (Late Early Pleistocene) rhinoceros from Pietrafitta (Perugia, Umbria, central Italy), with notes on the Pirro and Westerhoven rhinoceroses. Palaeontographia Italica 80, 25–50.
McClymont, E.L., Sosdian, S.M., Rosell-Melé, A., Rosenthal, Y., 2013. Pleistocene sea-surface temperature evolution: Early cooling, delayed glacial intensification, and implications for the mid-Pleistocene climate transition. Earth-Science Reviews 123, 173–193.
Melentis, J.K., 1966. Studien über fossile Vertebraten Griechenlands. 4.Die pleistozänen Nashörner des Beckens von Megalopolis in Peloponnes (Griechenland). Annales Géologiques des Pays Helléniques 16, 363–435.
Meli, R., 1896. Notizie sopra alcuni resti di mammiferi (ossa e denti isolati) quaternarii, rinvenuti nei dintorni di Roma. Bollettino della Società Geologica Italiana 15, 291–296.
Milli, S., Palombo, M.R., 2005. The high-resolution sequence stratigraphy and the mammal fossil record: a test in the Middle-Upper Pleistocene deposits of the Roman Basin (Latium, Italy). Quaternary International 126/128, 251–270.
Milli, S., Palombo, M.R., Petronio, C., Sardella, R., 2004. The Middle Pleistocene deposits of the Roman Basin (Latium, Italy): an integrated approach of mammal biochronology and sequence stratigraphy. Rivista Italiana di Paleontologia e Stratigrafia 110, 557–567.
Moullé, P.-E., Lacombat, F., Echassoux, A., 2006. Apport des grands mammifères de la grotte du Vallonnet (Roquebrune-Cap-Martin, Alpes-Maritimes, France) à la connaissance du cadre biochronologique de la seconde moitié du Pléistocène inférieur d'Europe. L'Anthropologie 110, 837–849.
Muttoni, G., Scardia, G., Kent, D.V., Swisher, C.C., Manzi, G., 2009. Pleistocene magnetochronology of early hominin sites at Ceprano and Fontana Ranuccio, Italy. Earth and Planetary Science Letters 286, 255–268.
Orlova, L.A., Kuzmin, Y.V., Dementiev, V.N., 2004. A review of the evidence for extinction chronologies for five species of upper Pleistocene megafauna in Siberia. Radiocarbon 46, 301–314.
Palmarelli, A., Palombo, M.R., 1981. Un cranio di *Coelodonta antiquitatis* (Blumenbach) (Rhinocerotidae) del Pleistocene superiore del Monte Circeo (Lazio meridionale). Bollettino Servizio Geologico d'Italia 102, 281–312.
Palombo, M.R., 2004. Biochronology of the Plio-Pleistocene mammalian faunas of Italian peninsula: knowledge, problems and perspective. Il Quaternario 17, 565–582.
Palombo, M.R., Azanza, B., Alberdi, M.T., 2002. Italian mammal biochronology from Latest Miocene to Middle Pleistocene: a multivariate approach. Geologica Romana 36, 335–368.
Palombo, M.R., Milli, S., Rosa, C., 2004. Remarks on the late Middle Pleistocene biochronology on the mammalian faunal complexes of the Campagna Romana. Geologica Romana 37, 135–143.
Palombo, M.R., Mussi, M., Agostini, S., Barbieri, M., Di Canzio, E., Di Rita, F., Fiore, I., Iacumin, P., Magri, D., Speranza, F., Tagliacozzo, A., 2010. Human peopling of Italian intramontane basins: the early Middle Pleistocene site of Pagliare di Sassa (L'Aquila, central Italy). Quaternary International 223–224, 170–178.
Pandolfi, L., 2011a. Il cranio di *Stephanorhinus hemitoechus* (Falconer, 1859) di Fosso Malafede (Vitinia, Roma) con note sulla prima presenza della specie in Italia. Il Quaternario 24, 25–32.
Pandolfi, L., 2011b. *Stephanorhinus kirchbergensis* (Jäger, 1839) from the Middle Pleistocene site of Riano (Roma, Central Italy). Il Quaternario 24, 103–112.
Pandolfi, L., 2013. Rhinocerotidae (Mammalia, Perissodactyla) from the Middle Pleistocene site of Ponte Milvio, Central Italy. Bollettino della Società Paleontologica Italiana 52, 219–229.
Pandolfi, L., Petronio, C., 2011. *Stephanorhinus etruscus* (Falconer, 1868) from Pirro Nord (Apricena, Foggia, Southern Italy) with notes on the other late Early Pleistocene rhinoceros remains of Italy. Rivista Italiana di Paleontologia e Stratigrafia 117, 173–187.
Pandolfi, L., Tagliacozzo, A., 2013. Earliest occurrence of Woolly Rhino (*Coelodonta antiquitatis*) in Italy (Late Pleistocene, Grotta Romanelli site). Rivista Italiana di Paleontologia e Stratigrafia 119, 125–129.
Pandolfi, L., Tagliacozzo, A., 2015. *Stephanorhinus hemitoechus* (Mammalia, Rhinocerotidae) from the Late Pleistocene of Valle Radice (Sora, Central Italy) and re-evaluation of the morphometric variability of the species in Europe. Geobios, http://dx.doi.org/10.1016/j.geobios.2015.02.002.
Pandolfi, L., Gaeta, M., Petronio, C., 2013a. The skull of *Stephanorhinus hemitoechus* (Mammalia, Rhinocerotidae) from the Middle Pleistocene of Campagna Romana (Rome, central Italy): biochronological and paleobiogeographic implications. Bulletin of Geosciences 88, 51–62.
Pandolfi, L., Grossi, F., Frezza, V., 2013b. A Miocene Acheratheriine Rhinocerotid (Mammalia, Perissodactyla) from Early Pleistocene marine deposits at Monte delle Piche (Rome, Central Italy). Rivista Italiana di Paleontologia e Stratigrafia 119, 401–405.
Pandolfi, L., Grossi, F., Frezza, V., 2015. New insights into the Pleistocene deposits of Monte delle Piche, Rome, and remarks on the biochronology of continental *Hippopotamus* (Mammalia, Hippopotamidae) and *Stephanorhinus etruscus* (Mammalia, Rhinocerotidae) in Italy. Estudios Geológicos 71 (1), e026, http://dx.doi.org/10.3989/egeol.41796.337.
Petronio, C., Sardella, R., 1998. Remarks on the stratigraphy and biochronology of the Late Pleistocene deposit of Ingarano (Apulia, Southern Italy). Rivista Italiana di Paleontologia e Stratigrafia 104, 287–294.
Petronio, C., Sardella, R., 1999. Biochronology of the Pleistocene mammal fauna from Ponte Galeria (Rome) and remarks on the Middle Galerian faunas. Rivista Italiana di Paleontologia e Stratigrafia 105, 155–164.
Petronio, C., Bellucci, L., Martinetto, E., Pandolfi, L., Salari, L., 2011. Biochronology and Palaeoenvironmental Changes from the Middle Pliocene to the Late Pleistocene in Central Italy. Geodiversitas 33, 485–517.
Ponzi, G., 1858. Sui lavori della strada ferrata di Civitavecchia da Roma alla Magliana. Atti dell'Accademia Pontificia de' Nuovi Lincei XI, 377–382.
Ponzi, G., 1878. Ossa fossili subappennine dei dintorni di Roma. Reale Accademia dei Lincei 2, 1–30.
Portis, A., 1896. Contribuzioni alla storia fisica del bacino di Roma e studi sopra l'estensione da darsi al Pliocene superiore. Vol. II, Roma. .
Portis, A., 1899. Una nuova specie di rinoceronti fossile in Italia? Bollettino della Società Geologica Italiana 18, 116–131.
Ravazzi, C., Pini, R., Breda, M., Martinetto, E., Muttoni, G., Chiesa, S., Confortini, F., Egli, R., 2005. The lacustrine deposits of Fornaci di Ranica (late Early Pleistocene, Italian Pre-Alps): stratigraphy, palaeoenvironment and geological evolution. Quaternary International 131, 35–58.
Ringström, T., 1924. Nashörner der *Hipparion*-Fauna Nord-Chinas. Palaeontologica Sinica, Series C 1, 1–159.
Schreiber, H.D., 2005. Osteological investigations on skeleton material of Rhinoceroses (Rhinocerotidae, Mammalia) from the early Middle Pleistocene locality of Mauer near Heidelberg (SW-Germany). Quaternaire hors série 2, 103–111.
Schreve, D.C., 1996. The mammalian fauna from the Waechter excavations, Barnfield Pit, Swanscombe. In: Conway, B., McNabb, J., Ashton, N. (Eds.), Excavations at Barnfield Pit, Swanscombe, 1968–1972. Occasional paper, 94. British Museum, London, pp. 149–162.
Sesé, C., Soto, E., 2005. Mamíferos del yacimiento del Pleistoceno Medio de Ambrona (Soria, España): Análisis faunístico e interpretación paleoambiental. In: Santonja, M., Pérez-González, A. (Eds.), Los yacimientos paleolíticos de Ambrona y Torralba (Soria). Un siglo de investigaciones arqueológicas, Zona Arqueológica 5, pp. 258–280.
Sorgi, C., 1994. La successione morfo-litostratigrafica in destra Tevere dell'ambito dell'evoluzione geologica quaternaria dell'area romana. Tesi di Laurea, Università degli Studi di Roma "La Sapienza" (unpublished).
Tong, H., Wu, X.Z., 2010. *Stephanorhinus kirchbergensis* (Rhinocerotidae, Mammalia) from the Rhino Cave in Shennongjia, Hubei. Chinese Science Bulletin 55, 1157–1168.
Toula, F., 1902. Das Nashörn von Hundsheim: *Rhinoceros* (*Ceratorhinus* Osborn) *hundsheimensis* nov. form.: mit Ausfuhrungen uber die Verhaltnisse von elf Schadeln von *Rhinoceros* (*Ceratorhinus*) *sumatrensis*. Abhandlungen der Geologischen Reichsanstalt 19, 1–92.
Vaufrey, R., 1927. Le mammouth et le rhinocéros à narines cloisonnées en Italie méridionale. Bulletin de la Societé Géologique Française 27, 163–171.
Ventriglia, U., 1971. La Geologia della Città di Roma. Amministrazione Provinciale, Roma.
Verri, A., 1915. Cenni spiegativi della Carta Geologica di Roma pubblicata dal R. Uff. Geologico su rilevamento del Tenente Generale A. Verri. Novara. Istituto Geografico De Agostini, Novara56.